Accepted Manuscript

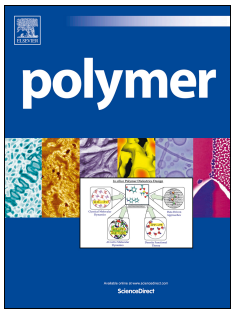

Effect of physical aging on the gas transport and sorption in PIM-1 membranes

M. Lanč, K. Pilnáček, O. Vopička, K. Friess, P. Bernardo, F. Bazzarelli, F. Tasselli, G. Clarizia, C.R. Mason, L. Maynard-Atem, P.M. Budd, D. Fritsch, YuP. Yampolskii, V. Shantarovich, J.C. Jansen

PII: S0032-3861(16)30952-1

DOI: 10.1016/j.polymer.2016.10.040

Reference: JPOL 19140

To appear in: *Polymer*

Received Date: 8 August 2016

Revised Date: 17 October 2016

Accepted Date: 18 October 2016

Please cite this article as: Lanč M, Pilnáček K, Vopička O, Friess K, Bernardo P, Bazzarelli F, Tasselli F, Clarizia G, Mason CR, Maynard-Atem L, Budd PM, Fritsch D, Yampolskii Y, Shantarovich V, Jansen JC, Effect of physical aging on the gas transport and sorption in PIM-1 membranes, *Polymer* (2016), doi: 10.1016/j.polymer.2016.10.040.

Effect of physical aging on the gas transport and sorption in PIM-1 membranes

M. Lanč[1], K. Pilnáček[1], O. Vopička[1], K. Friess[1*], P. Bernardo[2], F. Bazzarelli[2], F. Tasselli[2], G. Clarizia[2], C.R. Mason[3], L. Maynard-Atem[3], P.M. Budd[3*], D. Fritsch[4], Yu.P. Yampolskii[5], V. Shantarovich[6], J.C. Jansen[2*].

Graphical Abstract

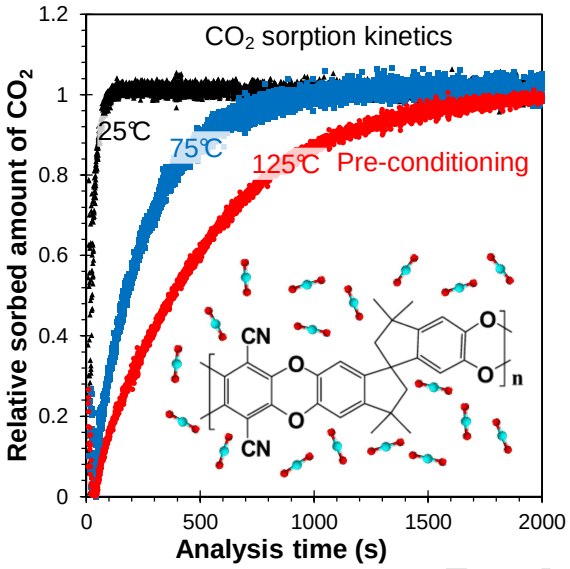

Effect of physical aging on the gas transport and sorption in PIM-1 membranes

M. Lanč[1], K. Pilnáček[1], O. Vopička[1], K. Friess[1*], P. Bernardo[2], F. Bazzarelli[2], F. Tasselli[2], G. Clarizia[2], C.R. Mason[3], L. Maynard-Atem[3], P.M. Budd[3*], D. Fritsch[4], Yu.P. Yampolskii[5], V. Shantarovich[6], J.C. Jansen[2*].

1. Department of Physical Chemistry, University of Chemistry and Technology, Technická 5, 166 28 Prague 6, Czech Republic
2. Institute on Membrane Technology (ITM-CNR), Via P. Bucci 17C, I-87036 Rende (CS), Italy
3. School of Chemistry, University of Manchester, Manchester, M13 9PL, UK
4. Fraunhofer-Institut für Angewandte Polymerforschung IAP, Geiselbergstr. 69, 14476 Potsdam, Germany
5. A.V. Topchiev Institute of Petrochemical Synthesis, 29 Leninsky Prospect, 119991, Moscow, Russian Federation
6. N.N. Semenov Institute of Chemical Physics, 4, Kosygina Str. Moscow, Russian Federation

*__Corresponding author:__ (JCJ) e-mail: johannescarolus.jansen@cnr.it, Tel:+39 0984 492031. (PMB) e-mail: peter.budd@manchester.ac.uk, Tel. +44 161 2754711; (KF) e-mail: karel.friess@vscht.cz, Tel. +420 220 444029.

Abstract

Understanding of the properties over long time scales is a key requirement for the successful application of novel polymers as membrane materials. In this light, the physical aging of dense PIM-1 films with different previous histories was monitored for more than 4 years via parallel gas sorption and permeability measurements. The effect of aging on the individual transport parameters, permeability, solubility and diffusivity, was studied on alcohol treated membranes with high excess free volume. Thermal conditioning of these membranes led to accelerated aging and a reduction of the initial gas permeability and diffusivity of the membranes. A long-term CO_2 sorption analysis showed aging affected the sorption kinetics much more than the total equilibrium sorption. This was confirmed by permeation studies with six different gases, showing that the reduction of the permeability coefficient of the samples as a function of time is almost entirely due to a reduction of the diffusion coefficient. A renewed alcohol treatment of the aged membrane led to significant rejuvenation of the membrane. To the best of our knowledge, this is the first systematic long term

aging study on PIM-1 via simultaneous analysis of sorption and permeation kinetics. Mixed gas permeation measurements with a CO_2/CH_4 mixture and an $N_2/O_2/CO_2$ mixture confirm the excellent permselective properties of the PIM-1 membranes even after long aging.

Keywords

PIM-1 membranes; Physical aging; Gas permeability; Gas sorption; Carbon dioxide

Introduction

Gas separation is involved in many chemical processes and engineering applications. Compared to conventional energy-intensive techniques, like pressure swing absorption and cryogenic distillation, membrane gas separation combines small footprint with high energy efficiency, large separation capability and ease of scale-up [1]. The introduction of efficient membrane separation systems could represent a solution for environmental challenges such as CO_2 capture to reduce global warming [2]. The reduction of global greenhouse gas emissions involves large gas volumes, and membrane processes based on high free volume polymers with a high permeability may offer a solution [3]. However, such polymers may be subject to strong aging phenomena, and in the case of membranes this is especially relevant if the selective layers are thin [4]. Therefore, a detailed study of their aging properties in relation to their gas separation performance on a time scale that is close enough to the normal life time of a membrane is crucial for their successful application.

Among high free-volume polymers, polymers of intrinsic microporosity (PIMs) possess good thermal and chemical stability. But the most attractive feature of this new class of polymers is their good combination of permeability coefficients and permselectivity. So, the data points of these polymers are located at or even above the Upper Bounds of the Robeson diagrams [5] for several important gas pairs (*e.g.*, O_2/N_2, CO_2/CH_4) [6]. The archetypal polymer PIM-1 (Scheme 1) has a rigid ladder polymer backbone with a spiro-centre site of contortion that produces sharp bends in the chain, resulting in a randomly contorted structure. These structural features prevent an efficient packing of the polymer in the solid state, leading to its great free volume and microporosity [7,8]. It is an organophilic, glassy polymer with no evidence of a glass transition temperature until the onset of thermal decomposition. An interesting feature of PIM-1 is that it has gas solubility coefficients higher than any other studied polymers, both glassy or rubbery [9]. Owing to the contorted structure, high molecular weight non-network PIMs are soluble in common organic solvents and can be solution-processed into free-standing membranes. Polymers that trap a large amount of interconnected free volume in the glassy state behave in many respects like microporous materials and potentially find application in membrane separations and heterogeneous catalysis [10]. A

feature of PIMs is their strong dependence of the gas permeation properties on the protocol of film formation and sample conditioning [9]. Residual solvents trapped inside PIM membranes are partly responsible for this behaviour [11], while the phenomena of swelling in non-solvents like alcohols can also play an important role as it happens in polyacetylenes [12].

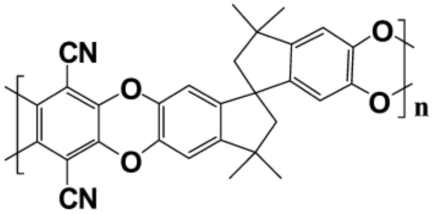

Scheme 1. Molecular structure of PIM-1.

Glassy polymers are non-equilibrium materials: over time, they lose excess free volume. This process, referred to as 'physical aging', results in a reduced gas permeability coupled often with an increased selectivity. Long-term aging can have a significant influence on the transport properties and represents a potential problem in the application of glassy polymer membranes. This can be particularly evident in the thin dense selective layer of composite or asymmetric membranes for gas separation [13,14]. Indeed, the ultra-high free volume polymer poly[1-(trimethylsilyl)-1-propyne] (PTMSP) did not find practical application as a gas separation membrane material because of its aging tendency and its sensitivity towards hydrocarbons [1].

Du *et al*. reported that PIM-1 membranes undergo a significant decline in permeability when exposed to condensable gases during the first 100 days of testing [15]. For example, the permeability declined to about 60% for CO_2 and 40% for CH_4, respectively. Thereafter, the aging rate slowed down and the permeabilities only varied 5-10% in the following 350 days. Staiger *et al.* studied the aging of PIM-1 films and showed that over a period of 140 hours, the permeability of individual gases declined between 20% (He) and 40% (CO_2) before the film failed [16]. Recently, Pilnacek *et al.* studied the aging of PIM-1 and PIM-EA-TB membranes and showed that the permeability of methanol decreased significantly during 650 hours and that this decline is more significant for continuous measurements, where the rearrangement of polymer chains is enhanced by the penetrant itself [17]. Long term aging studies on PIMs are rare in the literature. In a comprehensive study among different polymers of intrinsic microporosity, Swaidan et al. focused only on the effect of aging and plasticization on permeability.[18] They conclude that intra-chain rigidity is an important factor to determine whether a polymer has high permeability, but various factors determine its tendency towards aging. PALS measurements attributed the origin of the aging of PIM-1 to a collapse of the larger free volume elements. It has often been discussed that the gas

transport properties of glassy polymers depend on the amount and distribution of free volume and on chain mobility [19]. The rigid and contorted molecular structure of PIMs, which frustrates packing and creates free volume, is coupled with chemical functionality giving strong intermolecular interactions. This results in very high gas solubility and in relatively higher permeability coefficients than in many other polymer membranes. To investigate the origin of the high permeability, there has been a number of studies of PIM-1 by positron annihilation lifetime spectroscopy (PALS) [9,16,20–22]. This probing method showed a bimodal size distribution for PIM-1, like other highly permeable polymers, *e.g.* PTMSP or amorphous Teflons [23].

Commercial membranes for gas separation processes are usually in the form of composite membranes that consist of a porous substructure and a thin pore-free, dense polymer film. Such thin films may have significantly different behaviour from thick films for various polymers [24,25] and a greatly accelerated aging is observed in films with a thickness below 1 micron [4,26,27]. Accelerated aging is also found in thin film composites of PIMs [28]. Harms *et al*. confirmed the much faster aging in thin PIM-1 films compared to thick films via PALS studies with depth profiling [21]. They showed that even in relatively thin films of few microns the aging process may continue for several months, in which a slow migration of the FV elements towards the surface takes place. Small and wide angle x-ray diffraction studies underscore the unique structural features and the fundamental difference in the organization of free volume in these highly permeable polymers with respect to more conventional polymers [29]. This study hypothesizes a dual aging mechanism of PIMs, with two regimes of aging, interpreted as diffusion of pores to the surface of the membrane, and shrinkage of pores in time. In this work also heating of the samples will be shown to accelerate the aging process.

The effects of aging in PIM-1 films may be reversed by soaking the membrane in methanol, as already observed for PTMSP [30]. Methanol treatment removes residual casting solvent and permits relaxation of the PIM-1 chains and increases the free volume [9,12,31]. Weakly bonded alcohols with a small molecular size can be desorbed more easily at room temperature than the original casting solvent, leaving larger voids than in the as cast membrane. In contrast, water clusters require heating above 100 °C to desorb and above 160°C for their complete removal [32].

It is well known that the transport of gases through polymeric dense films can be described by the solution-diffusion mechanism [33]. The gas permeability, *P*, includes a thermodynamic component, the solubility coefficient, *S,* and a kinetic component, the diffusion coefficient, *D*:

$$P = D \cdot S \qquad \text{Eq. 1}$$

The gas solubility strongly depends on the free volume distribution and on the intramolecular interactions between penetrant and the polymer. The diffusivity of a penetrant molecule is mostly related to the mobility and the packing density of the polymer chains, as well as to its own dimensions. A large amount of free volume favours both the solubility and the diffusivity in a polymer. The time lag permeation technique has proven to be an effective method for characterisation of dense membranes, allowing a direct estimation of the permeability and diffusion coefficients via Eq. 1 [34,35]. This technique also allows an indirect determination of the solubility, but independent sorption measurements give more reliable results, especially in the case of anomalous transport behaviour.

So far, most aging studies focused on the time dependence of structural parameters such as free volume or the permeability. Very few studies dealt with the individual contributions of solubility and diffusivity to permeability, but none of these studies used a direct comparison of the transport parameters measured independently via permeation and sorption analysis. Therefore, the aim of the present work was to study the physical aging of dense PIM-1 membranes through a detailed analysis of gas permeation and sorption kinetics. Since alcohol soaking and thermal treatment is often reported to enhance the permeability of PIMs, while membranes will always be thin film composites with traces of residual solvent, both states are compared in this work.

Experimental

Materials

Chloroform, dichloromethane, n-hexane and ethanol, purchased from Carlo Erba Reagenti (Italy), were reagent grade and were used without further purification.

The gases for the permeation experiments (nitrogen, oxygen, methane, helium, hydrogen and carbon dioxide, all with a purity 99.999+%) were supplied by Pirossigeno, Italy.

Carbon dioxide for sorption experiments (99.99+%) was supplied by SIAD Czech.

Certified gas mixtures were supplied by Sapio at a purity of ±0.01% from the certified concentration (CO_2/CH_4 mixture with 47.89 mol.% CH_4 and $N_2/CO_2/O_2$ mixture with 10.10 mol.% CO_2 and 10.02 mol.% O_2), or the mixtures were prepared from the pure gases by in-line mixing with calibrated mass flow controllers (Bronkhorst).

Methods

Polymer preparation and characterization

PIM-1, batch LMA06, was prepared by the low temperature method as described previously [37]. For determination of the BET surface area, low-temperature (77 K) N_2 adsorption/desorption

measurements of powders were carried out using a Micromeritics ASAP2020 instrument. Samples were degassed for 16 h at 120 °C under high vacuum, then further degassed on the analysis port for 12 h at 120 °C.

Dense membrane preparation and post-treatment

Dense isotropic PIM-1 membranes were prepared by solvent evaporation. The polymer used (batch LMA06) has a weight-average molar mass, M_w, of 144,000 g mol^{-1} from multi-detector gel permeation chromatography (Viscotek VE2001 GPC solvent/sample module with two GMHHRM columns and a Viscotek TDA302 triple-detector array, chloroform as solvent at a flow rate of 1 cm^3 min^{-1}). A 5 wt.% PIM-1 solution was prepared in chloroform by magnetic stirring for at least 48 hours until a clear homogeneous solution was obtained. The solution was then filtered through a 40 μm metallic wire net. The films of PIM-1 were cast from the polymeric solution onto glass plates in metal casting rings. The solvent was gradually evaporated at room temperature, slowing down the evaporation by partially covering the casting ring. The membranes detached spontaneously from the glass support and were dried at room temperature and ambient pressure for several days. The thickness of the films was in the range of 80-110 μm, a range where the intrinsic properties are thickness-independent. The isotropic dense membranes were bright yellow transparent films, sufficiently flexible and robust to be handled without difficulties.

As a post-treatment step, the membranes were immersed in ethanol overnight and dried for one day at ambient conditions. This treatment resets the sample history and removes traces of residual casting solvent. An as-cast sample was tested as a reference without any specific treatment. The ethanol-soaked membranes were conditioned for 4 hours under vacuum at 25°C, 75°C and 125°C, respectively, to study the effect of the thermal history and to remove traces of the alcohol itself.

The samples used for the aging studies were stored in the air between the measurements, without any special conditions. The aged sample used for mixed gas permeation tests was treated as above and conditioned at 100°C, after which it was stored for over 5 years without intermediate permeation measurements.

Single gas permeability measurements

Permeation measurements were carried out with single gases at 25 °C and at a feed pressure of one bar. A fixed volume pressure increase setup, also known as time lag setup, was used. It is equipped with PC controlled pneumatic valves that allow response times of less than 0.5 s [38]. Before each experiment, each membrane sample was carefully evacuated with a rotary pump (10^{-2} mbar) to remove any dissolved species, including moisture from the air. The pump was equipped with an

activated alumina trap to avoid oil contamination of the membrane. The gases were tested in the following order: He, H_2, N_2, O_2, CH_4, and CO_2.

The measurements were carried out in the time lag mode [39], which allows for the determination of the diffusion coefficient of each gas through the membrane. The pressure in the fixed permeate volume was monitored by a pressure transducer, starting from the first exposure of the membrane to the feed gas. The following equation describes the time-pressure curve:

$$p_t = p_0 + \left(\mathrm{d}p/\mathrm{d}t\right)_0 \cdot t + \frac{RT \cdot A \cdot l}{V_P \cdot V_m} \cdot p_f \cdot S\left(\frac{D \cdot t}{l^2} - \frac{1}{6} - \frac{2}{\pi^2}\sum_1^\infty \frac{(-1)^n}{n^2}\exp\left(-\frac{D \cdot n^2 \cdot \pi^2 \cdot t}{l^2}\right)\right) \quad \text{Eq. 2}$$

where p_t is the permeate pressure at time t and p_0 is the starting pressure, typically less than 0.05 mbar. The baseline slope $(\mathrm{d}p/\mathrm{d}t)_0$ is normally negligible if the membrane is defect-free and sufficiently degassed. R is the universal gas constant, T the absolute temperature, A the exposed membrane area, l the membrane thickness, V_P the permeate volume, V_m the molar volume of a gas at standard temperature and pressure (0 °C and 1 atm), p_f the feed pressure, S the solubility and D the diffusion coefficient.

The permeability coefficient, P, is calculated from the slope of the curve in steady state condition:

$$p_t = p_0 + \left(dp/dt\right)_0 \cdot t + \frac{RT \cdot A}{V_P \cdot V_m} \cdot \frac{p_f \cdot P}{l}\left(t - \frac{l^2}{6D}\right) \quad \text{Eq. 3}$$

The last term corrects for the gas permeation time lag, Θ, which depends on the specific penetrant and on the membrane thickness

$$\Theta = \frac{l^2}{6\,D} \quad \text{Eq. 4}$$

The determination of Θ allows for the calculation of the diffusion coefficient of the penetrant, while the solubility of the gas in the polymer matrix is determined indirectly, via the equation:

$$S = \frac{P}{D} \quad \text{Eq. 5}$$

The ideal selectivity between two gases, obtained as the ratio of the individual single gas permeabilities, can be decoupled into solubility-selectivity and diffusivity-selectivity:

$$\alpha_{A/B} = \frac{P_A}{P_B} = \frac{S_A}{S_B} \cdot \frac{D_A}{D_B} \qquad \text{Eq. 6}$$

The exposed membrane area was 2.14 cm^2. The thickness of the isotropic dense films was determined before each measurement, using a digital micrometer (Mitutoyo).

Mixed gas permeability measurements

Mixed gas permeation experiments were carried out on a custom made constant pressure / variable volume instrument, equipped with a modified Millipore permeation cell (diameter 47 mm). The experiments were carried out at a feed flow rate of 100-200 cm^3 min^{-1} and a feed pressure of 0-5 bar(g), using EL-FLOW electronic Mass Flow Controllers (Bronkhorst) in the feed line and an EL-PRESS electronic back pressure controller (Bronkhorst) in the retentate line. Argon (30 cm^3 min^{-1}) was used as the sweeping gas at ambient pressure. The actual temperature and pressure were recorded to convert the measured flow rates to standard temperature and pressure conditions (STP, 1 atm at 0°C).

The permeate composition was determined with a Mass Spectrometric device equipped with a quadrupole mass filter (Hiden Analytical, HPR-20 QIC Benchtop residual gas analysis system, max. 200 AMU) and a sampling capillary with a typical flow rate of ca. 10-20 cm^3 min^{-1} at ambient pressure, depending on the gas sampled. The electron ionization energy was 70 eV and the gases were detected with the SEM ion detector. Nitrogen was detected at 14 AMU to avoid overlap of N_2 with the CO fragments from CO_2 at 28 AMU in CO_2/N_2 mixtures; methane was detected at 15 AMU (as CH_3) to avoid overlap of the molecular CH_4 peak with the O fragment from CO_2 at 16 AMU in the case of CO_2/CH_4 mixtures. All sensitivity ratios were previously calibrated against the weaker ^{36}Ar isotope at 36 AMU (ca. 0.3% abundancy). During the permeation experiments, this signal was used as the internal standard for calculation of the gas concentrations in the sweep/permeate. In all experiments, the stage cut was below 1%.

The test specimen was a 125 μm thick EtOH soaked PIM-1 sample, treated for 4h at 100°C and then aged untouched for 5.8 years. Before each analysis, the membrane was flushed for at least 1 hour at both sides with two independent argon streams until the MS signal was sufficiently stable. Subsequently, two experiments were carried out. In the first experiment, the argon flux at the feed side was replaced by the pure gas or gas mixture at atmospheric pressure (absolute pressure 1 bar(a))

to determine the time needed to reach steady state permeation. In the second experiment, the feed pressure was stepwise changed from 0-5 bar(g) and back, with sufficiently long time intervals to reach steady state permeation in each step. The background signals were determined just before switching from argon to the gas mixture at the feed side, and were subtracted from the measured signal during data processing.

All measured data were recorded with the MASsoft software package supplied with the mass spectrometer and with the FlowPlot software supplied with the pressure and mass flow controllers. The measured data were processed by a self-written elaboration program.

The mixed gas selectivity, $\alpha_{i/j}$ was evaluated as the ratio of the individually calculated gas permeances (Π_i) in the mixture:

$$\alpha_{CO_2/N_2} = \frac{\Pi_{CO_2}}{\Pi_{N_2}} \qquad \text{Eq. 7}$$

$$\alpha_{CO_2/CH_4} = \frac{\Pi_{CO_2}}{\Pi_{CH_4}} \qquad \text{Eq. 8}$$

where the individual gas permeance, Π_i, of the i^{th} species in the mixture is obtained as the ratio of its volumetric permeate flux, $Q^{Permeate}$, to the partial pressure difference between the feed and permeate sides, ΔP_i:

$$\Pi_i = \frac{x_i^{Permeate} Q^{Permeate}}{x_i^{Feed} p^{Feed} - x_i^{Permeate} p^{Permeate}} \qquad \text{Eq. 9}$$

in which x_i is the mole fraction of the i^{th} species, P^{Feed} and $P^{Permeate}$ are the total feed and permeate pressures, respectively. The permeate flux is the flow rate per unit area, defined as:

$$Q^{Permeate} = \frac{J^{Permeate}}{A} \qquad \text{Eq. 10}$$

The volumetric permeate flow rate, $J^{Permeate}$, is calculated from the known Argon sweep flow rate and from the measured composition of the permeate/sweep mixture.

Sorption analysis

Carbon dioxide sorption experiments were performed using a self-developed sorption apparatus equipped with a calibrated McBain quartz spiral balance with automatic detection of the sample-target-point position, using a CCD camera (Sony) [40]. The apparatus was located in an air box thermostated to (25.0±0.1) °C (Julabo F-250). The PIM-1 sample was appended at the end of the spiral balance in the glass measuring chamber, which was evacuated before the measurement to a pressure lower than 10^{-3} mbar by a rotary oil pump (Trivac D4B, Oerlikon Leybold). A Leybold oil mist filter prevented contamination of the measuring chamber by oil vapours from the pump with 99.99% efficiency. After exposure of the sample to the pre-thermostated gas at a known pressure, an automatic optical system (Neovision) monitored the elongation of the quartz spiral, until an equilibrium state was reached. The experimental procedure for gas sorption was described in detail elsewhere [40,41]. Sorption experiments were conducted with all three membranes separately in sequences taking ca. 1 day, comprising firstly two consecutive experiments at 1 bar, each followed by desorption step under vacuum until time-invariant mass of the sample was reached. Then, one run with a gradual increase of pressure from vacuum to 7 bar with steps of ca. 1 bar was performed without desorption between the incremental steps.

The experimental results were parameterized with the dual mode sorption model [42,43] which describes the equilibrium concentration of sorbed gas in glassy polymers as a function of pressure. This model distinguishes between penetrant molecules dissolved in the polymer matrix by ordinary dissolution process with a local concentration C_D, according to the Henry's law, and molecules trapped in the unrelaxed volume of a polymer matrix below the glass transition temperature with a concentration C_H as given by the Langmuir equation (monolayer). The total sorbate concentration, C, consists of two distinct terms, accounting for the Henry and Langmuir sorption, respectively:

$$C = C_D + C_H = k_D \cdot p + \frac{C_H^{'} \cdot b \cdot p}{1 + b \cdot p} \qquad \text{Eq. 11}$$

where k_D is the Henry law constant, C'_H the Langmuir sorption capacity constant, b the Langmuir affinity constant and p the sorbate pressure. The dual mode sorption parameters were calculated by a nonlinear least squares fit of the sorption data. The CO_2 solubility (sorption) coefficient S was calculated from the sample mass, m_M, and the equilibrium gas mass uptake, m_g, at the given equilibrium pressure, p_{eq}, which was set as close as possible 1 bar:

$$S = \frac{m_g}{m_M \cdot p_{eq}} \qquad \text{Eq. 12}$$

Otherwise, when the entire sorption isotherm was available, the solubility coefficient was calculated at exactly 1 bar using the fitted dual mode sorption parameters.

The diffusion coefficient, *D*, was calculated from the sorption kinetics data, using a previously reported model (Eq. 13 [44]) with a correction for the gradual increase of the relative pressure, p_{rel}, during filling of the measurement chamber (Eq. 14, in which ξ is a fitting parameter).

$$\frac{Q_t}{Q_\infty} = 1 - \exp(-\xi \cdot t) - \xi \cdot t \cdot \exp(-\xi \cdot t) - \frac{8}{\pi^2} \sum_{i=0}^{\infty} \left[\frac{1}{(2 \cdot i + 1)^2} \left(A \cdot \exp\left(-d \cdot t \cdot (2 \cdot i + 1)^2\right) + (C \cdot t - A) \cdot \exp(-\xi \cdot t) \right) \right] \qquad \text{Eq. 13}$$

with

$$A = \frac{\xi^2}{\xi^2 - 2 \cdot \xi \cdot d \cdot (2 \cdot i + 1)^2 + d^2 \cdot (2 \cdot i + 1)^4}$$

$$C = \frac{\xi^2}{d \cdot (2 \cdot i + 1)^2 - \xi}$$

$$d = \frac{\pi^2 \cdot D}{l^2}$$

$$p_{rel} = 1 - \exp(-\xi \cdot t) - \xi \cdot t \cdot \exp(-\xi \cdot t) \qquad \text{Eq. 14}$$

Results and discussion

For reliable results of the aging studies, it was important to guarantee a well-defined initial state of the polymer samples because it is known that, due to the non-equilibrium state of glassy polymers, their properties depend strongly on the thermo-mechanical history. Typically, the history of polymer films can be normalized by heating them above the glass transition temperature T_g [13,42], followed by controlled cooling. Since PIM-1 does not have a T_g below its onset of thermal degradation, owing to its extremely rigid ladder-like structure, an alternative procedure has to be considered. Soaking of polymers in a suitable solvent, which is able to swell but not dissolve them, also allows them to rearrange into a more relaxed state. This procedure was already reported for PIM membranes and was shown to have as a side effect a dramatic increase in the permeability [9].

Gas transport parameters

Since the gas transport properties of membranes depend on many factors, including sometimes the measurement technique itself, comparative studies under different conditions and by different methods are very important. It is also important not to focus only on permeability, but to distinguish the contribution of diffusion and of solubility in the transport. Therefore, the present work uses independent permeability and sorption measurements to determine the three fundamental transport parameters: permeability, diffusivity and solubility. The transport parameters from permeability measurements were obtained via the typical time lag analysis [39] (Figure 1A). The permeability coefficient was determined from the pseudo steady state pressure increase rate of the fixed volume permeate via Eq. 3, while the diffusion coefficient and the solubility were determined from Eq. 4 and Eq. 5, respectively. In comparison, the solubility is determined also from independent sorption analysis (Eq. 12), while an alternative diffusion coefficient is calculated from the sorption kinetics curve via Eq. 13 (Figure 1B).

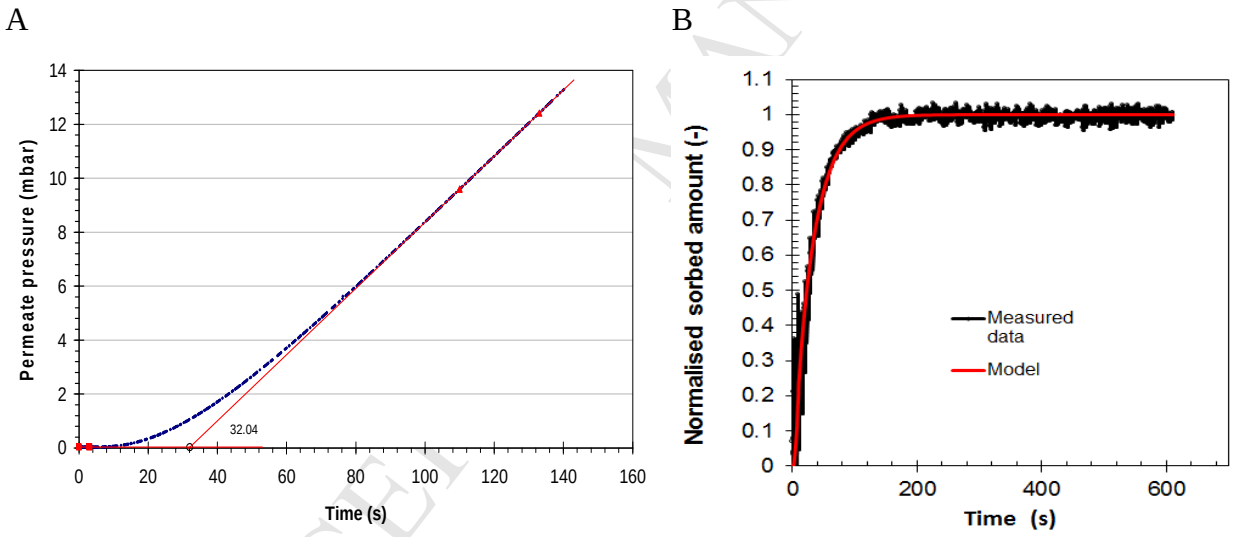

Figure 1. Typical experimental curves for the determination of the CO_2 transport parameters from the permeability measurements, using the time lag method [39] (A) and from sorption kinetics measurements, using a diffusion model with dynamic pressure correction [44] (B). Analysis temperature 25°C, feed pressure 1 bar)

The permeability shows a strong increase upon alcohol soaking, followed by a gradual decrease in time. The transport parameters of the PIM-1 membrane treated at 25 °C before and after ethanol soaking are summarized in Table 1. The diffusion coefficient decreases in the order: He > H_2 >> O_2 > CO_2 ≈ N_2 ≈> CH_4, according to their crescent kinetic diameters. This is typical size sieving and is characteristic for diffusion of weakly interacting species in a stiff glassy polymer matrix. This order

remains the same after soaking in EtOH and after aging of the sample. Carbon dioxide is by far the most permeable species. This is rather unusual for size sieving glassy polymer membranes, but it is a typical characteristic of the polymers of intrinsic microporosity [9], known for their exceptionally high CO_2 solubility.

Table 1. Pure gas permeability (*P*) and diffusion coefficient (*D*) with the corresponding selectivities of a representative dense PIM-1 membrane at 25°C, as determined by time lag analysis.[a]

			P **(Barrer)** [c]			***D*** **(10^{-8} cm^2 s^{-1})**		
Gas	**d_{eff} (Å)** [b]	**State** [d]	A	B	C	A	B	C
N_2	3.04		280	857	125	83	178	26.7
H_2	2.14		1740	4500	2440	>2680	>5060	>3080
He	1.78		758	1706	1140	>4350	>7050	>5280
O_2	2.89		742	2200	600	202	526	116
CH_4	3.18		410	1150	159	29	67.3	8.7
CO_2	3.02		4970	13300	2840	81	198	43.8
			***P*/*P*$_{N2}$ (-)**			***D*/*D*$_{N2}$ (-)**		
Gas	**d_{eff} (Å)** [b]	**State** [d]	A	B	C	A	B	C
N_2	3.04		-	-	-	-	-	-
H_2	2.14		6.21	5.25	19.4	32.4	28.5	115
He	1.78		2.71	1.99	9.10	52.6	39.7	198
O_2	2.89		2.65	2.57	4.79	2.44	2.96	4.34
CH_4	3.18		1.47	1.34	1.27	0.35	1.34	0.33
CO_2	3.02		17.8	15.52	22.7	0.98	1.11	1.64

[a] PIM-1 Batch LMA06. Temperature = 25 °C, Feed pressure = 1 bar.

[b] Effective diameter defined by Teplyakov *et al.* [45]

[c] 1 Barrer = 10^{-10} cm^3 (STP) cm cm^{-2} cmHg^{-1} s^{-1}

[d] A = Fresh, as cast sample (ca. 90 μm), B = Ethanol treated sample at 25 °C (ca. 110 μm), C = Ethanol treated sample, aged for 1200 days.

One hypothesis often mentioned for the increase of the permeability upon alcohol treatment is the removal of traces of residual solvent, which may obstruct [38] or otherwise influence [11] the gas transport in the as-cast membrane. In the present work, a significant increase in the membrane thickness and a simultaneous lateral contraction was observed after alcohol treatment and subsequent drying (Figure S 6.). After the initial increase of the thickness, there is no clear further change as a function of aging time. This indicates that the membrane assumes a more relaxed state upon swelling, apparently by plasticization of the highly rigid PIM chains. A similar effect was also observed by Emmler *et al*. after a methanol treatment [31], where the asymmetric expansion of the

PIM-1 films was also attributed to chain relaxation by methanol. Apparently, the solution casting procedure induces anisotropy in the polymer film. Such an effect was previously observed for membranes based on the perfluoropolymer Hyflon AD [46]. McDermott *et al*. observed distinct differences in the X-ray diffraction pattern of PIM-1 after methanol soaking, in the small distance range, and they tentatively attributed this to changes in the pore size [47]. Interestingly, their WAXS pattern does not only show the typical amorphous halo, but also a smooth shoulder which is not present in nonporous polymers. In addition, some small peaks at distances of 0.89, 1.25 and 1.63 Å, superimposed on this shoulder, must be attributed to intersegmental distances of the monomeric units in the highly rigid polymer chain.

The effect of aging on permeability is better seen in Figure 2. This figure shows the permeability of the as cast and the ethanol treated sample as a function of time for almost 4 years. In addition to the results of the regularly treated sample, the figure also shows the permeability of two samples, heated for 4 hours under vacuum at 75°C and 125°C just after the ethanol treatment. All samples show a gradual decrease of permeability as a function of time. This behaviour makes permeability measurements by far the most valuable technique to probe the physical aging in PIM-1, much more sensitive than PALS and specific volume or density analysis. The stepwise increase of the 75°C sample and the 125°C sample around 200 days show the 'rejuvenation' of the film by renewed EtOH soaking. Remarkably, the 'as cast' membrane showed an increasing permeability for helium and hydrogen over time. Most likely this is because this sample still contains some residual solvent, that is gradually removed in the repeated vacuum cycles during testing. Upon solvent removal from the as-cast sample, two effects occur simultaneously: the loss of solvent leads to an increase of free volume, but the simultaneous rearrangement leads to an increase in selectivity and a decrease in permeability. The net effect is different for small and large molecules, and apparently only for the small molecules is the effect on the permeability positive, because smaller channels need to be created for them to be able to diffuse. Therefore, the permeability for small molecules increases, while for large molecules the reduction of the free volume over time dominates and causes a net reduction of their permeability.

This is different from what happens in the case of alcohol treatment and subsequent aging. In that case, three different effects take place. There is a general increase of the excess free volume by swelling of the polymer matrix and a simultaneous liberation of free volume by removal of traces of residual solvent, both leading to a major increase in the permeability of all gases. The third effect is the lattice contraction and rearrangement of the free volume upon aging, leading to a gradual decrease in permeability and an increase in selectivity. The latter is much more evident in the alcohol treated samples after the creation of a large excess free volume. Indeed, PALS analysis

revealed that the observed decrease in gas permeability in PIM-1 as the result of physical aging is primarily due to the collapse of the larger pores [16], enhancing the size sieving behaviour. The increase in helium and hydrogen permeability and the decrease of the permeability of the other gases, leads to a significant increase in, for instance, the H_2/CH_4 and H_2/N_2 selectivities in the 'as cast' sample upon aging.

For the aging of the three alcohol treated samples, the trend in permeability is more or less linear on a log-log scale, similar to what was already discussed by Zhou *et al.* for fluoropolyimide films [48]. Thus, the influence of physical aging on the permeability can be approximated by the following equation:

$$P = P_0 \cdot t^{-\beta_P} \quad \text{or} \quad \log P = \log P_0 - \beta_P \cdot \log t \qquad \text{Eq. 15}$$

Where P_0 is the initial permeability at t=1 and β_P has the physical meaning of a permeability aging rate constant. Although this equation becomes mathematically meaningless if t=0, in real situations this will never occur because a finite time is always needed to bring the sample into a representative starting condition for the aging studies. The permeability decreases mostly during the first several days and then gradually slows down. This 'self-retarding' feature of the physical aging was previously described for other glassy polymers [13,24,49]. Lattice contraction was identified as the dominant mechanism for relatively thick PIM-1 films (> 1 μm) by Harms *et al.* via depth-resolved PALS analysis, while simultaneous hole diffusion was suggested for thinner films [21]. SAXS/WAXS studies by McDermott *et al.* also suggested two distinct aging mechanisms, namely free volume contraction and free volume diffusion, respectively, and in their case the latter mechanism was visible at thicknesses below ca. 100 μm [29]. The present samples were all sufficiently thick for free volume contraction to be the dominant mechanism. As already seen for a single sample in Table 1, an identical time dependency of permeability is seen for the diffusion coefficient, whereas the solubility as determined from the time lag experiments is constant within the experimental error (Figure S 3 and Figure S 4). Thus, the trend in the diffusion coefficient can be described by an analogous equation:

$$D = D_0 \cdot t^{-\beta_D} \quad \text{or} \quad \log D = \log D_0 - \beta_D \cdot \log t \qquad \text{Eq. 16}$$

Where D_0 is the initial diffusion coefficient at t = 1 and β_D has the physical meaning of a diffusivity aging rate constant.

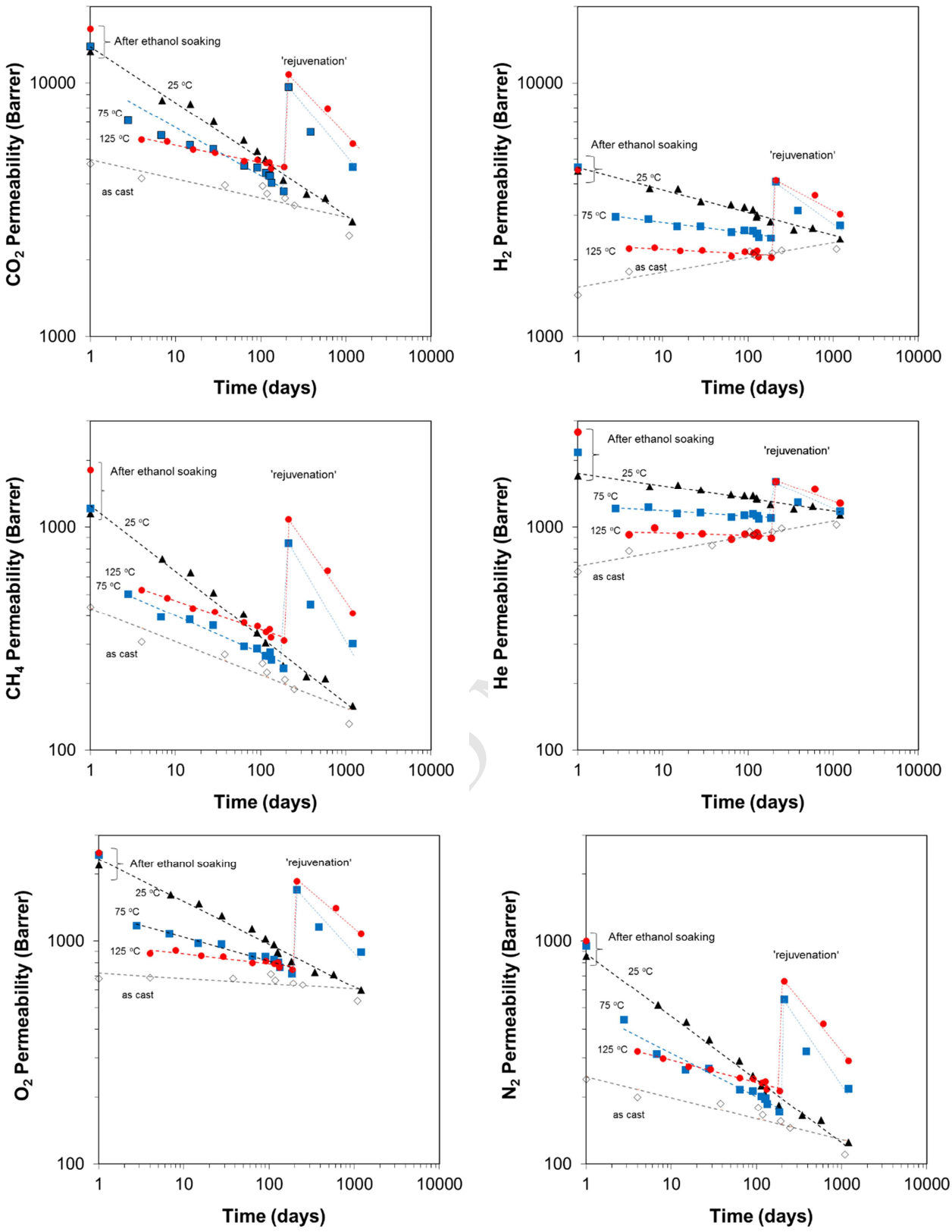

Figure 2. Permeability change at 25°C over time for PIM-1 dense films with different histories. Three samples were ethanol soaked and then thermally conditioned at 25 (▲), 75 (■) and 125 °C (●), respectively. An additional untreated sample was followed during time (◇). The dotted lines represent the fitting of the experimental data with Eq. 15.

Whereas in the present case Eq. 15 describes the aging process particularly well, Rowe et al. described the permeability of PSf membranes by the commonly used Struik model for physical aging [50] and found log-linear behaviour over a quite broad time range [51] after a slower initial decrease of permeability for thicker films. Only for thin films and very long times, the permeability decrease deviated from the log-linear behaviour. This was also confirmed by Müller et al. [52], via predictions with the Struik model to very long times, leading to a similar trend as observed by us for PIM-1. This confirms that the time scales for physical aging of PIM-1 are clearly much faster than for common low FFV polymers.

Figure 3 shows a plot of the permeability aging rate constants as a function of the effective diameters of the six gases, obtained by fitting of the experimental permeability data with Eq. 15. The aging rate constant increases exponentially with the square of the effective diameter of the gases, which indicates that the aging affects large molecules much stronger than small molecules. This figure demonstrates quantitatively the lower aging rate for the samples that were treated at higher temperatures after the ethanol soaking.

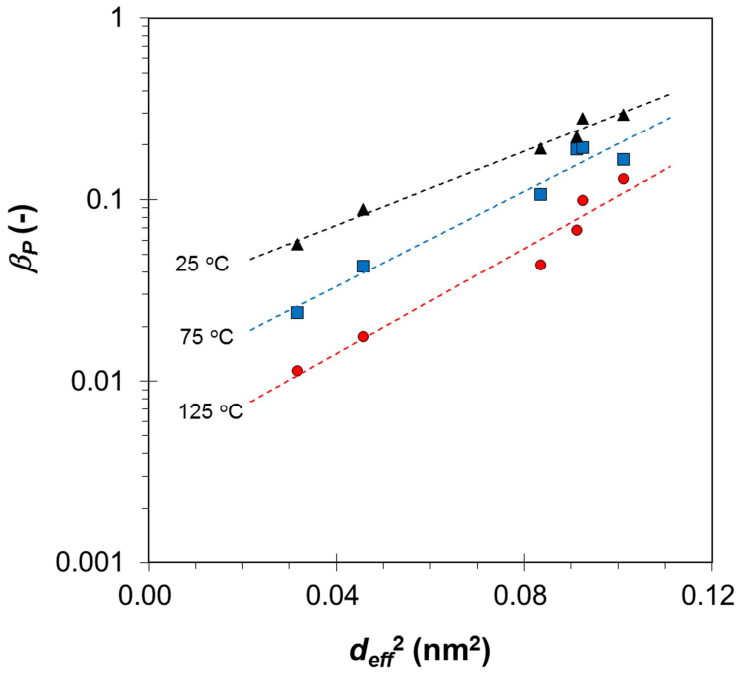

Figure 3. Correlation of the permeability aging rate constant β_P, obtained by fitting of the experimental permeability data with Eq. 15, with the square of the permeant effective diameter [45] for the PIM-1 samples having different histories. Three samples were ethanol soaked and then thermally conditioned at 25 (▲), 75 (■) and 125 C° (●), respectively. The dashed lines represent a least squares fit with an exponential curve.

Independent gravimetric sorption measurements with CO_2 confirm that there is no significant change in the gas solubility as a function of the aging time and there is also no clear difference among the samples conditioned at higher temperature after the ethanol soaking (Figure 4). The only difference in sorption behaviour among all samples is the relatively low CO_2 solubility in the as cast membrane, where part of the free volume is still occupied by the residual solvent. Combining Eq. 5, Eq. 15 and Eq. 16 gives for the solubility aging rate constant, β_S,:

$$\beta_S = \beta_P - \beta_D \qquad \text{Eq. 17}$$

The constant solubility as a function of time (Figure 4A) means that the solubility aging rate constant (Eq. 17) is equal to zero. This indeed shows that β_P and β_D must be equal, and thus that the decrease in permeability upon aging is entirely controlled by the decrease in diffusivity, as discussed above.

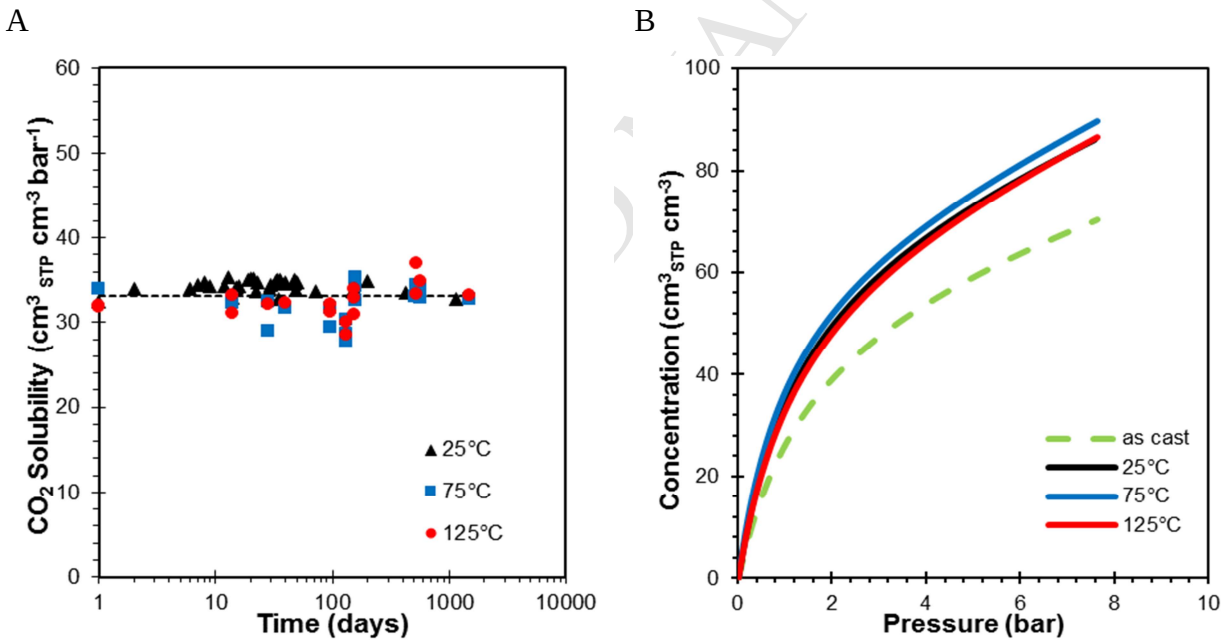

Figure 4. A) Equilibrium CO_2 sorption coefficients, *S*, at 1 bar and 25°C as a function of the aging time. The dashed line represents the average of the solubility. B) CO_2 sorption isotherms in the as cast and the ethanol- and heat-treated PIM-1 membranes, calculated by the Dual Mode sorption model (Eq. 11). The curves of the alcohol treated samples are calculated from the Dual Mode parameters averaged over the entire aging time interval while that of the as cast sample represents a single measurement.

The sorption kinetics data confirm the dramatic effect of aging on the diffusion coefficient (Figure 5). The thermally treated samples exhibited substantially slower kinetics due to the much lower diffusion coefficients of the samples heated to 75°C and 125°C. This is a result of the enhanced aging during the thermal treatment. The diffusion coefficient further decreases as a function of time, as discussed on the basis of the diffusion data obtained from the permeability experiments. The CO_2 diffusion coefficient obtained from sorption kinetics measurements move in an almost parallel fashion on a log-log scale for the three samples treated at different temperatures after ethanol soaking (Figure 5B). This trend is remarkably different from that of the CO_2 permeability, which becomes nearly similar for all samples after long aging (Figure 2). This is because of fundamental differences in the conditions of the sorption and permeation experiments. In the latter, the permeate side of the membrane is always at very low pressure (<10 mbar), at which the material is not affected by the presence of the gas. In contrast, in sorption experiments, the entire membrane is exposed to the higher CO_2 pressure, and dilation induced by the CO_2 sorption itself limits the collapse of the free volume to some extent. This trend is remarkably similar to that of the helium and hydrogen permeability (Figure 2), for which it was already shown that the permeability aging rate constant is much lower (Figure 3).

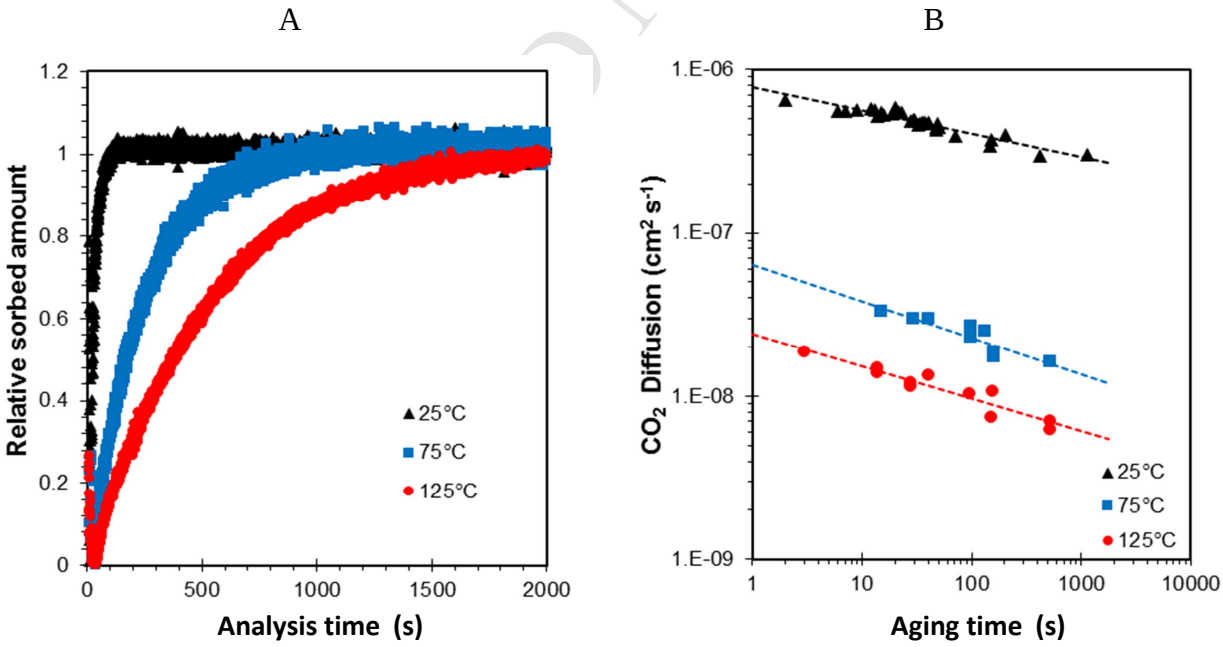

Figure 5. (A) Comparison of CO_2 sorption kinetics at 1 bar and 25°C in PIM-1 samples treated at different temperatures after alcohol soaking. (B) Diffusion coefficient, calculated from the sorption kinetics curves (Eq. 13) as a function of aging time. The dotted lines represent the fitting of the experimental data with Eq. 16.

Whereas the permeability for most gases becomes almost independent of the previous history after long aging times, the permeability of helium and hydrogen remains significantly different, depending on the thermal treatment. This suggests that the interconnection of the free volume for these small molecules changes much less than for the larger ones, and that this interconnection depends much more on the thermal treatment than on the subsequent aging. This is compatible with the results of the modelling studies, which demonstrated that simulated swelling results in an increase of the free volume element size, whereas no changes occur in closely packed associated chains upon swelling [53]. The thermal treatment affects the degree of association of the closely packed chains and this does not change substantially in later stages as a function of time or after exposure to the gases.

A similar study on the aging of PTMSP claimed that the decrease in the permeability coefficient was dependent on the decrease in the hole saturation constant of Langmuir adsorption (C'_H) [30], which is related to the volume of the microvoids [54]. In contrast, the present study showed that neither the thermal treatment nor the aging during the studied period induced evident changes in the Langmuir (C'_H) or Henry (k_D) parameters (Figure S 5). This suggests that the narrower micropore size distributions of PIM-1 compared to PTMSP [55] only undergoes some rearrangement upon aging and not a strong overall reduction of the void volume. The Langmuir parameters mostly reflect the nearly constant internal surface area, while the strong decrease in diffusion reflects a reduction of the overall void volume and especially the reduction of the microvoid interconnectivity. It can be assumed that connectivity of free volume elements in PIM-1 is less than in PTMSP, as confirmed by a comparison of visualization of free volume models in these two polymers [56]. No experimental methods exist, which can accurately determine the pore interconnectivity and only such molecular modelling approaches can provide this information.

The conditioning at higher temperature partially eliminates the effect of the alcohol treatment, reducing the initial permeability, as well as the rate of the subsequent aging (Figure 2). At the same time, the thermal treatment increases the selectivity of the films. Thus, thermal treatment induces an accelerated aging, which stabilizes the sample in time. Indeed, heating below the glass transition increases the density of glassy polymers [57–59], which is the process that takes place during aging. The samples treated at 75 °C and 125 °C were soaked in ethanol again after ca. 200 days and this resulted in a significant permeability recovery (Figure 2). The new permeability was slightly lower than the original value of the ethanol-treated samples. Interestingly, after the second soaking the aging rate was much lower and the permeability remained far above the value of the as cast membrane over long times.

Overall membrane performance

The Robeson diagrams in Figure 6 show the effect of ethanol soaking and physical aging on the selectivity of the PIM-1 membranes for four relevant gas pairs: CO_2/CH_4, O_2/N_2, CO_2/N_2 and H_2/N_2. The ethanol treatment increases the gas permeability and decreases the ideal selectivity very much according to the typical trade-off behaviour [5].

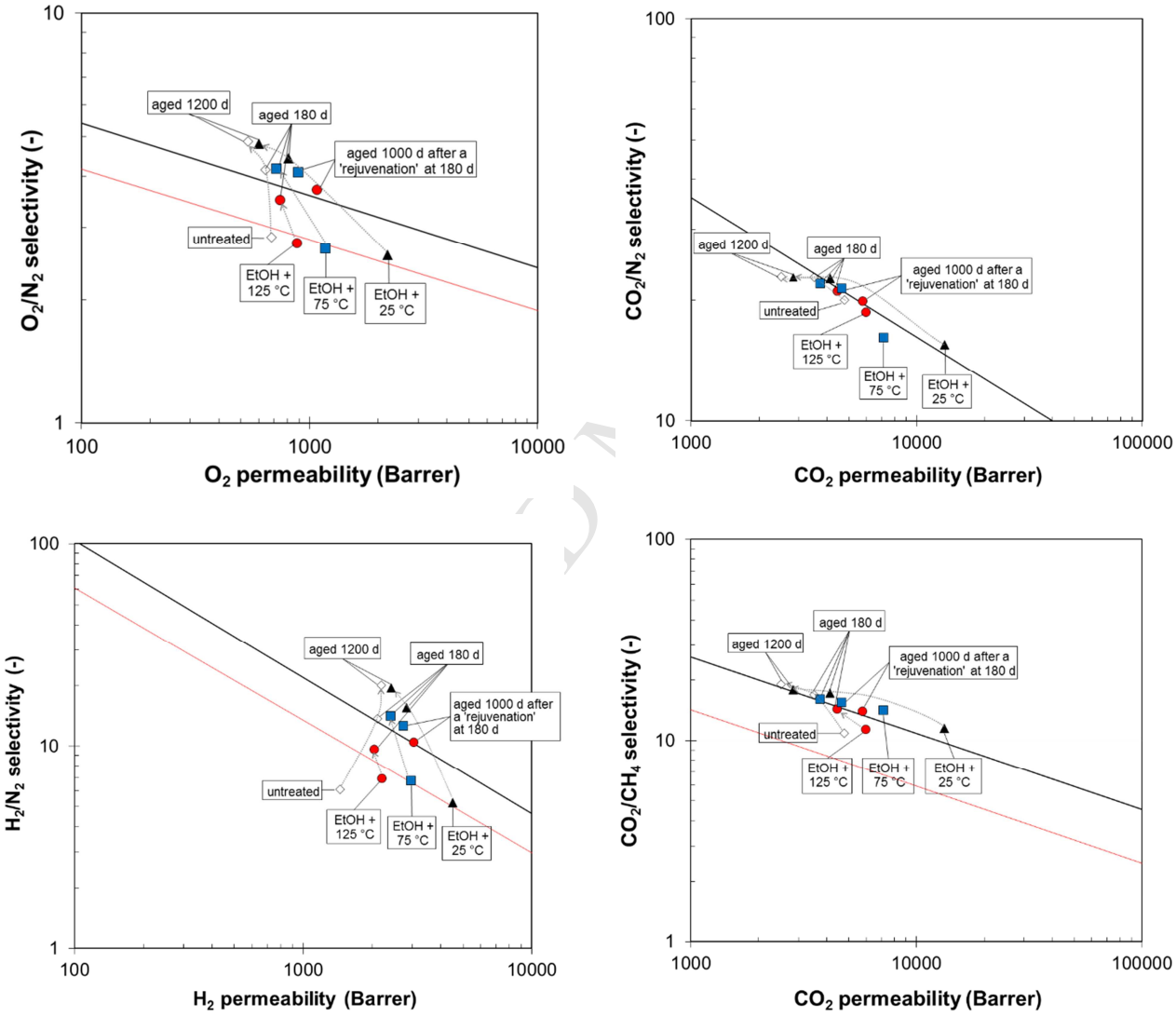

Figure 6. Robeson diagrams for a number of relevant gas pairs [5]. Circles: samples after the treatment (time 0); triangles: samples aged for ca. 180 days. Three samples were ethanol soaked and then thermally conditioned at 25 (▲), 75 (■) and 125 °C (●), respectively. An additional sample not treated was followed during time (◇). The red and black lines represent the 1991 and 2008 Robeson upper bounds, respectively [5].

Aging changes the gas permeability and selectivity in the opposite directions for the CO_2/N_2 and CO_2/CH_4 gas pairs, which move almost parallel to the Robeson 2008 upper bound. For the O_2/N_2 and H_2/N_2 gas pairs, the decrease in permeability is accompanied by a relatively large increase in selectivity, lifting the aged samples above the 2008 upper bound. In contrast to what is usually observed, the increase in hydrogen permeability of the as cast sample upon aging is also accompanied by a simultaneous increase in selectivity. Therefore, the H_2/N_2 gas pair shows the most remarkable increase in performance upon aging, moving perpendicularly to the Robeson upper bound. Recently, Lau et al. suggested a heat treatment on mixed matrix membranes, with as the main effect an increase of the selectivity and with relatively little change in permeability [60]. The underlying phenomenon is probably the same, and the presence of highly porous fillers guarantees an even higher permeability in their case.

The present work shows that all different treatment methods push the samples on different time scales to end conditions with very similar properties.

Mixed gas permeation properties

Preliminary gas separation tests were carried out with two gas mixtures, consisting of $N_2/O_2/CO_2$ in the ratio 79.88/10.02/10.10 mol%, and CO_2/CH_4 in the ratio of 52.1/47.9 mol%. The sample used was ethanol-soaked like the other samples and then dried at 100°C for 4 h and aged for >5 years. Therefore its behaviour should lie between that of the samples treated at 75°C and 125°C and then aged. In a single measurement run, the pressure was stepwise increased from 0 to 5 bar(g) with integer pressure values, and then stepwise decreased with half integer values. The results are given in Figure 7, which shows that for both gas mixtures, the permeability of each gas is nearly constant over the pressure range used. There is only a small decrease in CO_2 permeability as a function of pressure due to the dual mode behaviour.

The selectivity of these samples ($CO_2/CH_4 \approx 20$ and $CO_2/N_2 \approx 30$) at a CO_2 permeability near 3000 Barrer is completely in line with or even slightly better than the ideal selectivity (SI Table S1 and Table S2). This means that in the given pressure range the PIM-1 samples maintain their permselective properties excellently. Upon a close look at the permeation data, one can observe a weak hysteresis effect, with slightly lower permeabilities for the pressure increase run (integer pressures values) and slightly higher permeabilities in the subsequent pressure decrease run (half integer values). This is an indication of weak dilation of the sample, induced by the dissolved gases, which does not fully relax the original state and thus leads to a slightly higher permeability and consequently lower selectivity in the pressure decrease run. At low pressures this effect is small and does not affect the membrane performance substantially.

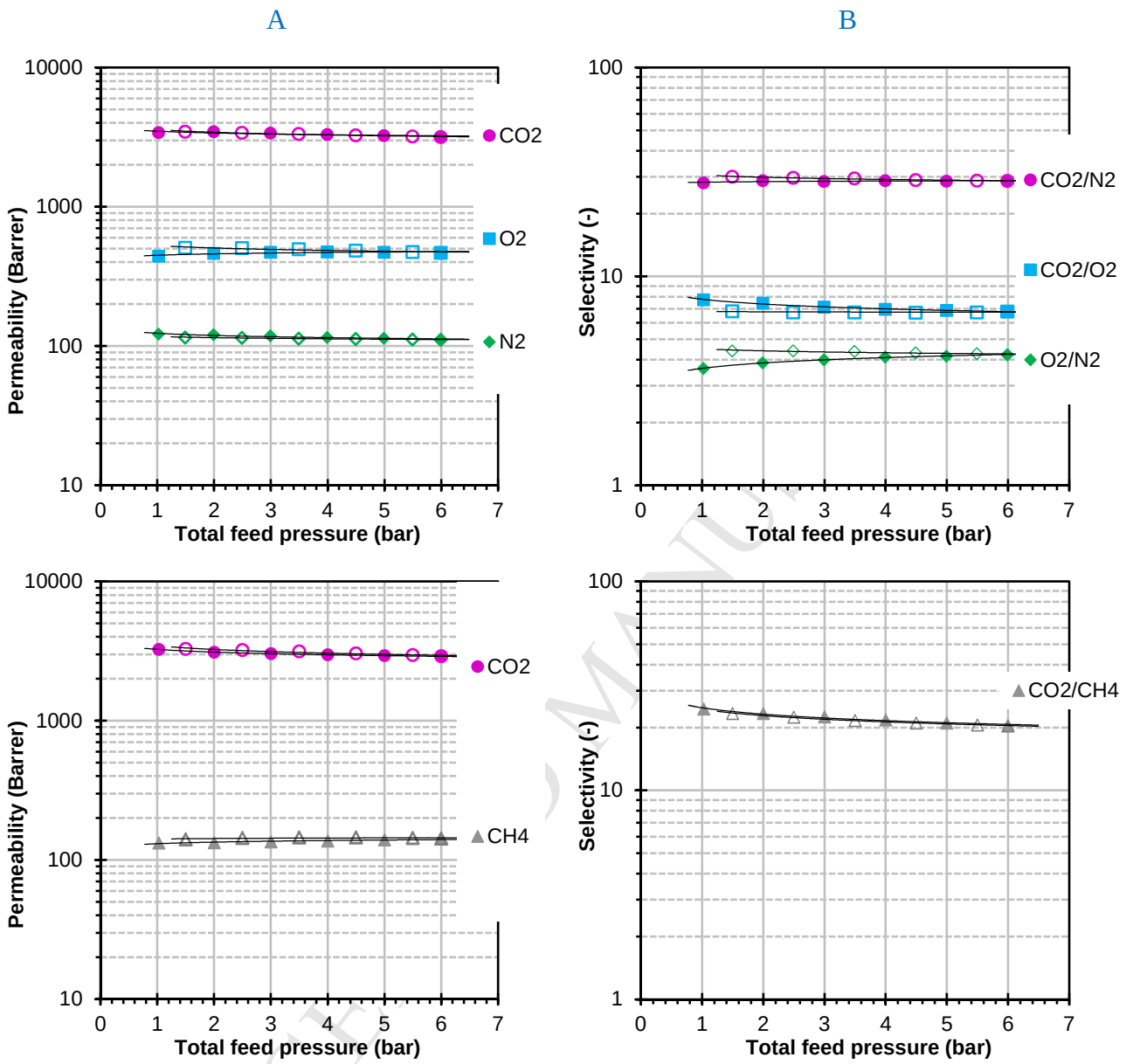

Figure 7. Mixed gas permeability (A) and selectivity (B) at 25°C for two gas feed streams, consisting of (top) a mixture of $N_2/O_2/CO_2$ in the ratio 79.88/10.02/10.10 mol%, and (bottom) a mixture of CO_2/CH_4 in the ratio of 52.1/47.9 mol%. Test sample: EtOH-soaked PIM-1 sample, treated for 4 h at 100°C and then aged untouched for 5.8 years, thickness 125.4 µm. Filled symbols at integer pressure values and open symbols at half integer values for the pressure increase and the pressure decrease run, respectively.

Conclusions

For the first time, independent long-term sorption and permeation studies of PIM-1 membranes revealed the nature of the decreasing permeability during aging. The measurements revealed that

the decrease of permeability during aging depends mainly on the reduction of the diffusion coefficient, while it is hardly affected by the solubility of the gas in the polymer matrix. Thanks to their very short response times and high precision, the quartz spring sorption balance and time lag permeation instrument, used in the present work, were able to follow the very quick kinetics of sorption and permeation in the PIM-1 samples.

Ethanol treatment partially cancels the previous history of PIM-1 membranes by removing residual solvent and relaxing stresses accumulated during the film formation. This results in a higher permeability for permanent gases, due to a strong increase in the diffusion coefficient and a small increase in the solubility. The aging-induced changes in the transport properties can be limited by a thermal treatment. The conditioning of ethanol-treated samples under vacuum at high temperature accelerates the aging and stabilizes the sample, guaranteeing a much lower further reduction of permeability in time.

In most cases, the alcohol treated samples follow the typical Robeson trade-off behaviour, but for the O_2/N_2 and H_2/N_2 gas pairs the physical aging leads to an increase of the membrane performance above the Robeson upper bound. This is because the molecules with the larger kinetic diameter are affected more by the physical aging than the smaller molecules, which is quantitatively expressed by a higher physical aging rate constant for permeation. In as cast membranes, the permeability of helium and hydrogen increases as a function of time due to the removal of residual solvent.

Renewed soaking of an aged membrane ‘rejuvenates’ the sample and restores most of its original permeability. A beneficial side-effect is that further aging after this step is slower than in the original sample. This may be an approach to counteract the effect of aging in thin films, where the phenomenon is normally much faster.

As a general conclusion, the present work demonstrates that aging of PIM-1 membranes mainly affects the diffusion coefficient of permanent gases, and hardly their solubility. At different but sufficiently long time scales, all treatment methods push the samples towards similar end conditions where the permselective properties hardly depend on the previous sample history. In addition, sorption of CO_2 at high pressure partially counteracts the effect of physical aging, which could be beneficial for practical application of these membranes. Mixed gas permeation experiments on an aged sample (>5 years) confirm that the good separation performance of this polymer is maintained over time for important separations operating at moderate pressures, such as CO_2 removal from flue gas or from biogas.

Acknowledgements

The work leading to these results has received funding from the European Community's Seventh Framework Programme (FP7/2007-2013) under grant agreements no. 228631, project *DoubleNanoMem* - "Nanocomposite and Nanostructured Polymeric Membranes for Gas and Vapour Separations" and no. 608490, project M^4CO_2 - "Energy efficient MOF-based Mixed-Matrix Membranes for CO_2 capture"

LMA received support from EPSRC grant EP/G065144/1

References

[1] P. Bernardo, E. Drioli, G. Golemme, Membrane gas separation: A review/state of the art, Ind. Eng. Chem. Res. 48 (2009) 4638–4663. doi:10.1021/ie8019032.

[2] A. Brunetti, F. Scura, G. Barbieri, E. Drioli, Membrane technologies for CO2 separation, J. Memb. Sci. 359 (2010) 115–125. doi:10.1016/j.memsci.2009.11.040.

[3] T.C. Merkel, H. Lin, X. Wei, R. Baker, Power plant post-combustion carbon dioxide capture: An opportunity for membranes, J. Memb. Sci. 359 (2010) 126–139. doi:10.1016/j.memsci.2009.10.041.

[4] P.H. Pfromm, The Impact of Physical Aging of Amorphous Glassy Polymers on Gas Separation Membranes, in: Mater. Sci. Membr. Gas Vap. Sep., 2006: pp. 293–306. doi:10.1002/047002903X.ch11.

[5] L.M. Robeson, The upper bound revisited, J. Memb. Sci. 320 (2008) 390–400. doi:10.1016/j.memsci.2008.04.030.

[6] P.M. Budd, K.J. Msayib, C.E. Tattershall, B.S. Ghanem, K.J. Reynolds, N.B. McKeown, et al., Gas separation membranes from polymers of intrinsic microporosity, J. Memb. Sci. 251 (2005) 263–269. doi:10.1016/j.memsci.2005.01.009.

[7] P.M. Budd, B.S. Ghanem, S. Makhseed, N.B. McKeown, K.J. Msayib, C.E. Tattershall, Polymers of intrinsic microporosity (PIMs): robust, solution-processable, organic nanoporous materials., Chem. Commun. (Camb). 10 (2004) 230–231. doi:10.1039/b311764b.

[8] P.M. Budd, N.B. McKeown, Highly permeable polymers for gas separation membranes, Polym. Chem. 1 (2010) 63–68. doi:10.1039/b9py00319c.

[9] P.M. Budd, N.B. McKeown, B.S. Ghanem, K.J. Msayib, D. Fritsch, L. Starannikova, et al., Gas permeation parameters and other physicochemical properties of a polymer of intrinsic microporosity: Polybenzodioxane PIM-1, J. Memb. Sci. 325 (2008) 851–860. doi:10.1016/j.memsci.2008.09.010.

[10] P.M. Budd, N.B. McKeown, D. Fritsch, Free volume and intrinsic microporosity in

polymers, J. Mater. Chem. 15 (2005) 1977–1986. doi:10.1039/b417402j.

[11] L. Zhang, W. Fang, J. Jiang, Effects of residual solvent on membrane structure and gas permeation in a polymer of intrinsic microporosity: Insight from atomistic simulation, J. Phys. Chem. C. 115 (2011) 11233–11239. doi:10.1021/jp2029888.

[12] A.J. Hill, S.J. Pas, T.J. Bastow, M.I. Burgar, K. Nagai, L.G. Toy, et al., Influence of methanol conditioning and physical aging on carbon spin-lattice relaxation times of poly(1-trimethylsilyl-1-propyne), J. Memb. Sci. 243 (2004) 37–44. doi:10.1016/j.memsci.2004.06.007.

[13] Y. Huang, X. Wang, D.R. Paul, Physical aging of thin glassy polymer films: Free volume interpretation, J. Memb. Sci. 277 (2006) 219–229. doi:10.1016/j.memsci.2005.10.032.

[14] Y. Huang, D.R. Paul, Effect of film thickness on the gas-permeation characteristics of glassy polymer membranes, Ind. Eng. Chem. Res. 46 (2007) 2342–2347. doi:10.1021/ie0610804.

[15] N. Du, M.M.D.- Cin, I. Pinnau, A. Nicalek, G.P. Robertson, M.D. Guiver, Azide-based cross-linking of polymers of intrinsic microporosity (PIMs) for condensable gas separation., Macromol. Rapid Commun. 32 (2011) 631–6. doi:10.1002/marc.201000775.

[16] C.L. Staiger, S.J. Pas, A.J. Hill, C.J. Cornelius, Gas separation, free volume distribution, and physical aging of a highly microporous spirobisindane polymer, Chem. Mater. 20 (2008) 2606–2608. doi:10.1021/cm071722t.

[17] K. Pilnáček, O. Vopička, M. Lanč, M. Dendisová, M. Zgažar, P.M. Budd, et al., Aging of polymers of intrinsic microporosity tracked by methanol vapour permeation, J. Memb. Sci. 520 (2016) 895–906. doi:http://dx.doi.org/10.1016/j.memsci.2016.08.054.

[18] R. Swaidan, B. Ghanem, E. Litwiller, I. Pinnau, Physical Aging, Plasticization and Their Effects on Gas Permeation in “rigid” Polymers of Intrinsic Microporosity, Macromolecules. 48 (2015) 6553–6561. doi:10.1021/acs.macromol.5b01581.

[19] A.Y. Alentiev, Y.P. Yampolskii, Free volume model and tradeoff relations of gas permeability and selectivity in glassy polymers, J. Memb. Sci. 165 (2000) 201–216. doi:10.1016/S0376-7388(99)00229-X.

[20] P.M. Budd, N.B. McKeown, D. Fritsch, Y. Yampolskii, V. Shantarovich, Gas Permeation Parameters and Other Physicochemical Properties of a Polymer of Intrinsic Microporosity (PIM-1), in: Membr. Gas Sep., John Wiley & Sons, Ltd, 2010: pp. 29–42. doi:10.1002/9780470665626.ch2.

[21] S. Harms, K. Rätzke, F. Faupel, N. Chaukura, P.M. Budd, W. Egger, et al., Aging and Free Volume in a Polymer of Intrinsic Microporosity (PIM-1), J. Adhes. 88 (2012) 608–619. doi:10.1080/00218464.2012.682902.

[22] R. Lima de Miranda, J. Kruse, K. Rätzke, F. Faupel, D. Fritsch, V. Abetz, et al., Unusual temperature dependence of the positron lifetime in a polymer of intrinsic microporosity, Phys. Status Solidi – Rapid Res. Lett. 1 (2007) 190–192. doi:10.1002/pssr.200701116.

[23] Y. Yampolskii, V. Shantarovich, Positron Annihilation Lifetime Spectroscopy and Other Methods for Free Volume Evaluation in Polymers, in: Mater. Sci. Membr. Gas Vap. Sep., John Wiley & Sons, Ltd, A. V. Topchiev Institute of Petrochemical Synthesis, Russian Academy of Sciences, 29 Leninsky Prospekt, Moscow 117912, Russian Federation, 2006: pp. 191–210. doi:10.1002/047002903X.ch6.

[24] M.S. McCaig, D.R. Paul, Effect of film thickness on the changes in gas permeability of a glassy polyarylate due to physical aging: Part I. Experimental observations, Polymer (Guildf). 41 (2000) 629–637. doi:10.1016/S0032-3861(99)00172-X.

[25] Y. Huang, D.R. Paul, Physical aging of thin glassy polymer films monitored by gas permeability, Polymer (Guildf). 45 (2004) 8377–8393. doi:10.1016/j.polymer.2004.10.019.

[26] P.H. Pfromm, W.J. Koros, Accelerated physical aging of thin glassy polymer films: evidence from gas transport measurements, Polymer (Guildf). 36 (1995) 2379–2387. doi:10.1016/0032-3861(95)97336-E.

[27] B.W. Rowe, B.D. Freeman, D.R. Paul, Influence of previous history on physical aging in thin glassy polymer films as gas separation membranes, Polymer (Guildf). 51 (2010) 3784–3792. doi:10.1016/j.polymer.2010.06.004.

[28] D. Fritsch, About Aging of Thin–film Composite Membranes, Procedia Eng. 44 (2012) 821–822. doi:10.1016/j.proeng.2012.08.585.

[29] A.G. McDermott, P.M. Budd, N.B. McKeown, C.M. Colina, J. Runt, Physical aging of polymers of intrinsic microporosity: a SAXS/WAXS study, J. Mater. Chem. A. 2 (2014) 11742–11752. doi:10.1039/C4TA02165G.

[30] K. Nagai, A. Higuchi, T. Nakagawa, Gas permeability and stability of poly(1-trimethylsilyl-1-propyne-co-1-phenyl-1-propyne) membranes, J. Polym. Sci. Part B Polym. Phys. 33 (1995) 289–298. doi:10.1002/polb.1995.090330214.

[31] T. Emmler, K. Heinrich, D. Fritsch, P.M. Budd, N. Chaukura, D. Ehlers, et al., Free volume investigation of polymers of intrinsic microporosity (PIMs): PIM-1 and PIM1 copolymers incorporating ethanoanthracene units, Macromolecules. 43 (2010) 6075–6084. doi:10.1021/ma1008786.

[32] Y. Yampolskii, A. Alentiev, G. Bondarenko, Y. Kostina, M. Heuchel, Intermolecular Interactions: New Way to Govern Transport Properties of Membrane Materials, Ind. Eng. Chem. Res. 49 (2010) 12031–12037. doi:10.1021/ie100097a.

[33] J.G. Wijmans, R.W. Baker, The solution-diffusion model: a review, J. Memb. Sci. 107 (1995) 1–21. doi:10.1016/0376-7388(95)00102-I.

[34] S.W. Rutherford, D.D. Do, Review of time lag permeation technique as a method for characterisation of porous media and membranes, Adsorption. 3 (1997) 283–312. doi:10.1007/BF01653631.

[35] S. Matteucci, Y. Yampolskii, B.D. Freeman, I. Pinnau, Transport of Gases and Vapors in Glassy and Rubbery Polymers, in: Y. Yampolskii, I. Pinnau, B.D. Freeman (Eds.), Mater. Sci. Membr. Gas Vap. Sep., John Wiley & Sons, Ltd, 2006: pp. 1–48. doi:10.1002/047002903X.ch1.

[36] D. Fritsch, P. Merten, K. Heinrich, M. Lazar, M. Priske, High performance organic solvent nanofiltration membranes: Development and thorough testing of thin film composite membranes made of polymers of intrinsic microporosity (PIMs), J. Memb. Sci. 401–402 (2012) 222–231. doi:10.1016/j.memsci.2012.02.008.

[37] P.M. Budd, E.S. Elabas, B.S. Ghanem, S. Makhseed, N.B. McKeown, K.J. Msayib, et al., Solution-Processed, Organophilic Membrane Derived from a Polymer of Intrinsic Microporosity, Adv. Mater. 16 (2004) 456–459. doi:10.1002/adma.200306053.

[38] C.R. Mason, L. Maynard-Atem, N.M. Al-Harbi, P.M. Budd, P. Bernardo, F. Bazzarelli, et al., Polymer of Intrinsic Microporosity Incorporating Thioamide Functionality: Preparation and Gas Transport Properties, Macromolecules. 44 (2011) 6471–6479. doi:10.1021/ma200918h.

[39] J. Crank, The mathematics of diffusion, 2nd ed., Clarendon Press, Oxford, 1975.

[40] K. Friess, V. Hynek, M. Šípek, W.M. Kujawski, O. Vopička, M. Zgažar, et al., Permeation and sorption properties of poly(ether-block-amide) membranes filled by two types of zeolites, Sep. Purif. Technol. 80 (2011) 418–427. doi:10.1016/j.seppur.2011.04.012.

[41] O. Vopička, K. Friess, V. Hynek, P. Sysel, M. Zgažar, M. Šípek, et al., Equilibrium and transient sorption of vapours and gases in the polymer of intrinsic microporosity PIM-1, J. Memb. Sci. 434 (2013) 148–160. doi:10.1016/j.memsci.2013.01.040.

[42] W.J. Koros, D.R. Paul, CO2 sorption in poly(ethylene terephthalate) above and below the glass transition, J. Polym. Sci. Polym. Phys. Ed. 16 (1978) 1947–1963. doi:10.1002/pol.1978.180161105.

[43] W.R. Vieth, K.J. Sladek, A model for diffusion in a glassy polymer, J. Colloid Sci. 20 (1965) 1014–1033. doi:10.1016/0095-8522(65)90071-1.

[44] O. Vopička, V. Hynek, M. Zgažar, K. Friess, M. Šípek, A new sorption model with a dynamic correction for the determination of diffusion coefficients, J. Memb. Sci. 330 (2009)

51–56. doi:10.1016/j.memsci.2008.12.037.

[45] V. Teplyakov, P. Meares, Correlation aspects of the selective gas permeabilities of polymeric materials and membranes, Gas Sep. Purif. 4 (1990) 66–74. doi:10.1016/0950-4214(90)80030-O.

[46] M. Macchione, J.C. Jansen, G. De Luca, E. Tocci, M. Longeri, E. Drioli, Experimental analysis and simulation of the gas transport in dense Hyflon® AD60X membranes: Influence of residual solvent, Polymer (Guildf). 48 (2007) 2619–2635. doi:10.1016/j.polymer.2007.02.068.

[47] A.G. McDermott, G.S. Larsen, P.M. Budd, C.M. Colina, J. Runt, Structural characterization of a polymer of intrinsic microporosity: X-ray scattering with interpretation enhanced by molecular dynamics simulations, Macromolecules. 44 (2011) 14–16. doi:10.1021/ma1024945.

[48] C. Zhou, T.S. Chung, R. Wang, S.H. Goh, A governing equation for physical aging of thick and thin fluoropolyimide films, J. Appl. Polym. Sci. 92 (2004) 1758–1764. doi:10.1002/app.20136.

[49] B.W. Rowe, L.M. Robeson, B.D. Freeman, D.R. Paul, Influence of temperature on the upper bound: Theoretical considerations and comparison with experimental results, J. Memb. Sci. 360 (2010) 58–69. doi:10.1016/j.memsci.2010.04.047.

[50] L.C.E. Struik, Physical Aging in Amorphous Polymers and Other Materials, Elsevier Scientific Publishing Company, 1978.

[51] B.W. Rowe, B.D. Freeman, D.R. Paul, Physical aging of ultrathin glassy polymer films tracked by gas permeability, Polymer (Guildf). 50 (2009) 5565–5575. doi:10.1016/j.polymer.2009.09.037.

[52] N. Müller, U.A. Handge, V. Abetz, Physical ageing and lifetime prediction of polymer membranes for gas separation processes, J. Memb. Sci. 516 (2016) 33–46. doi:10.1016/j.memsci.2016.05.055.

[53] K.E. Hart, J.M. Springmeier, N.B. McKeown, C.M. Colina, Simulated swelling during low-temperature N2 adsorption in polymers of intrinsic microporosity., Phys. Chem. Chem. Phys. 15 (2013) 20161–9. doi:10.1039/c3cp53402b.

[54] T. Nakagawa, T. Watanabe, M. Mori, K. Nagai, Aging of Gas Permeability in Poly[1-(trimethylsilyl)-1-propyne] (PTMSP) and PTMSP-Poly(tert-butylacetylene) Blends, in: Polym. Membr. Gas Vap. Sep., American Chemical Society, 1999: pp. 5–68. doi:doi:10.1021/bk-1999-0733.ch005.

[55] M. Heuchel, D. Fritsch, P.M. Budd, N.B. McKeown, D. Hofmann, Atomistic packing model

and free volume distribution of a polymer with intrinsic microporosity (PIM-1), J. Memb. Sci. 318 (2008) 84–99. doi:10.1016/j.memsci.2008.02.038.

[56] D. Hofmann, M. Entrialgo-Castano, A. Lerbret, M. Heuchel, Y. Yampolskii, Molecular modeling investigation of free volume distributions in stiff chain polymers with conventional and ultrahigh free volume: Comparison between molecular modeling and positron lifetime studies, Macromolecules. 36 (2003) 8528–8538. doi:10.1021/ma034971l.

[57] H. Shamsipur, B.A. Dawood, P.M. Budd, P. Bernardo, G. Clarizia, J.C. Jansen, Thermally Rearrangeable PIM-Polyimides for Gas Separation Membranes, Macromolecules. 47 (2014) 5595–5606. doi:10.1021/ma5011183.

[58] A.H. Chan, D.R. Paul, Influence of history on the gas sorption, thermal, and mechanical properties of glassy polycarbonate, J. Appl. Polym. Sci. 24 (1979) 1539–1550. doi:10.1002/app.1979.070240615.

[59] A.H. Chan, D.R. Paul, Effect of Sub-Tg Annealing on CO2 Sorption in Polycarbonate, Polym. Eng. Sci. 20 (1980) 87–94. doi:10.1002/pen.760200115.

[60] C.H. Lau, P.T. Nguyen, M.R. Hill, A.W. Thornton, K. Konstas, C.M. Doherty, et al., Ending aging in super glassy polymer membranes, Angew. Chemie - Int. Ed. 53 (2014) 5322–5326. doi:10.1002/anie.201402234.

Supplementary information

BET Surface area

A typical feature of microporous materials such as PIMs is their high surface area. Nitrogen sorption isotherms of a fresh 100 mg PIM-1 powder sample (batch LMA06) and two samples soaked in alcohol overnight are given in Figure S 1. The corresponding apparent BET surface area of the fresh sample was calculated as 685 m^2 g^{-1}. This value was found to be highly sensitive to alcohol treatment, increasing to 759 m^2 g^{-1} and 788 m^2 g^{-1} after ethanol and methanol treatment, respectively.

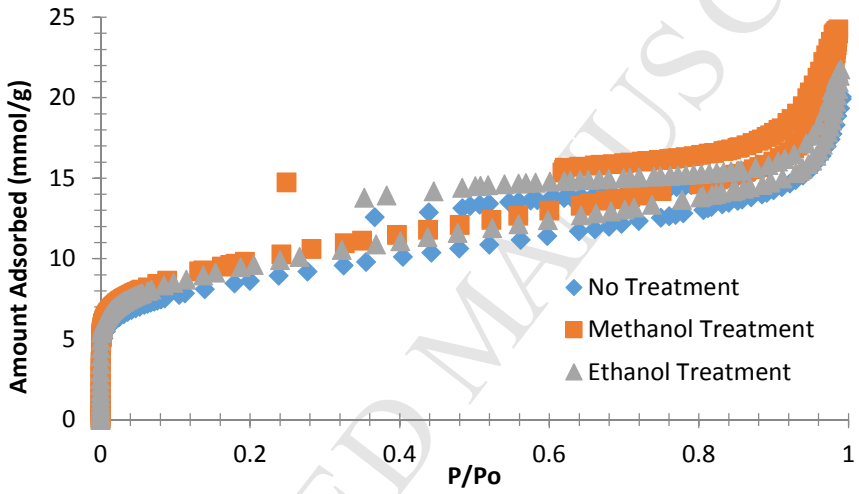

Figure S 1. N_2 sorption isotherms at 77 K for a PIM-1 powder sample as obtained from the synthesis and workup procedure (= without alcohol treatment) and after alcohol treatment.

The apparent BET surface area of a 12-week old PIM-1 sample shows a marked decrease when compared to the fresh PIM-1 powder (Figure S 2). After MeOH treatment, the BET surface area returns to an even higher value. The initial value of the original powder is lower than that of the freshly methanol-treated sample, probably because of its previous history during polymer preparation, isolation and storage. The increase in BET surface area from the fresh sample to the alcohol treated sample reflects the opening of pores that were previously unavailable to N_2 probe molecules. Swelling of the polymer by the alcohol causes a volume expansion of the material, which does not collapse entirely upon quick drying. Furthermore, additional voids may be opened due to the removal of material that has been adsorbed by the polymer during storage. Similarly, it was reported that methanol-treated PIM-1 samples have a higher free volume, because upon

methanol swelling the chain structure is relaxed from film forming stress and also because residual solvent and/or sorbed vapours are removed [1].

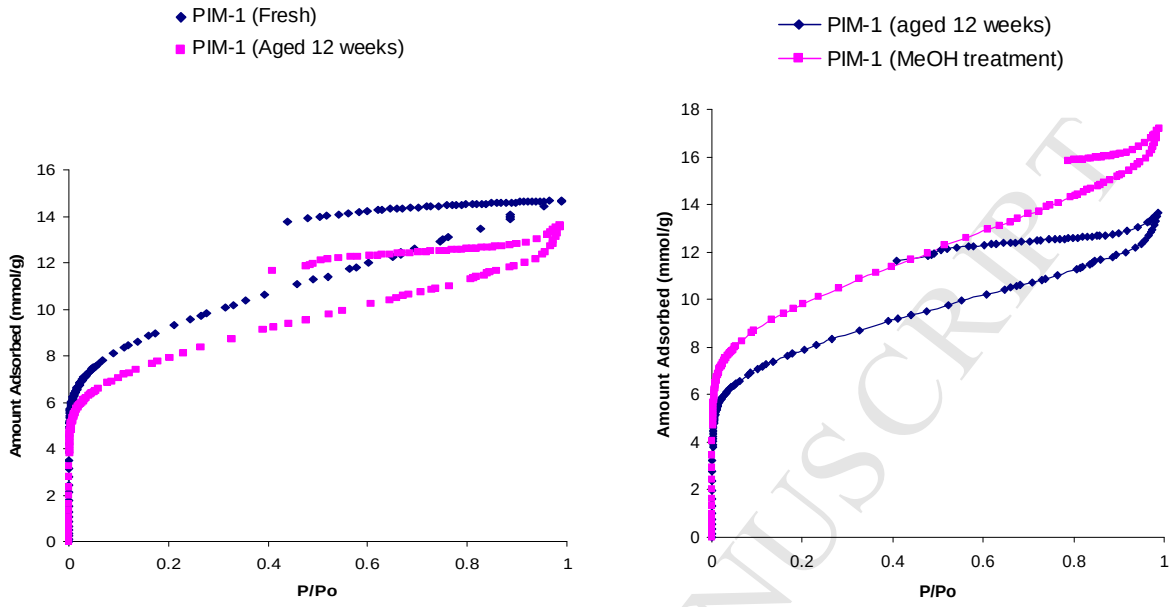

Figure S 2. Nitrogen sorption isotherms at 77 K comparing freshly prepared PIM-1 to an aged sample of the same polymer (left) and sorption isotherms of the same before and after renewed MeOH treatment (right).

Figure S 3 shows the diffusion coefficient, *D*, as a function of the aging time for three ethanol soaked samples and an as cast membrane as obtained by time lag measurements.

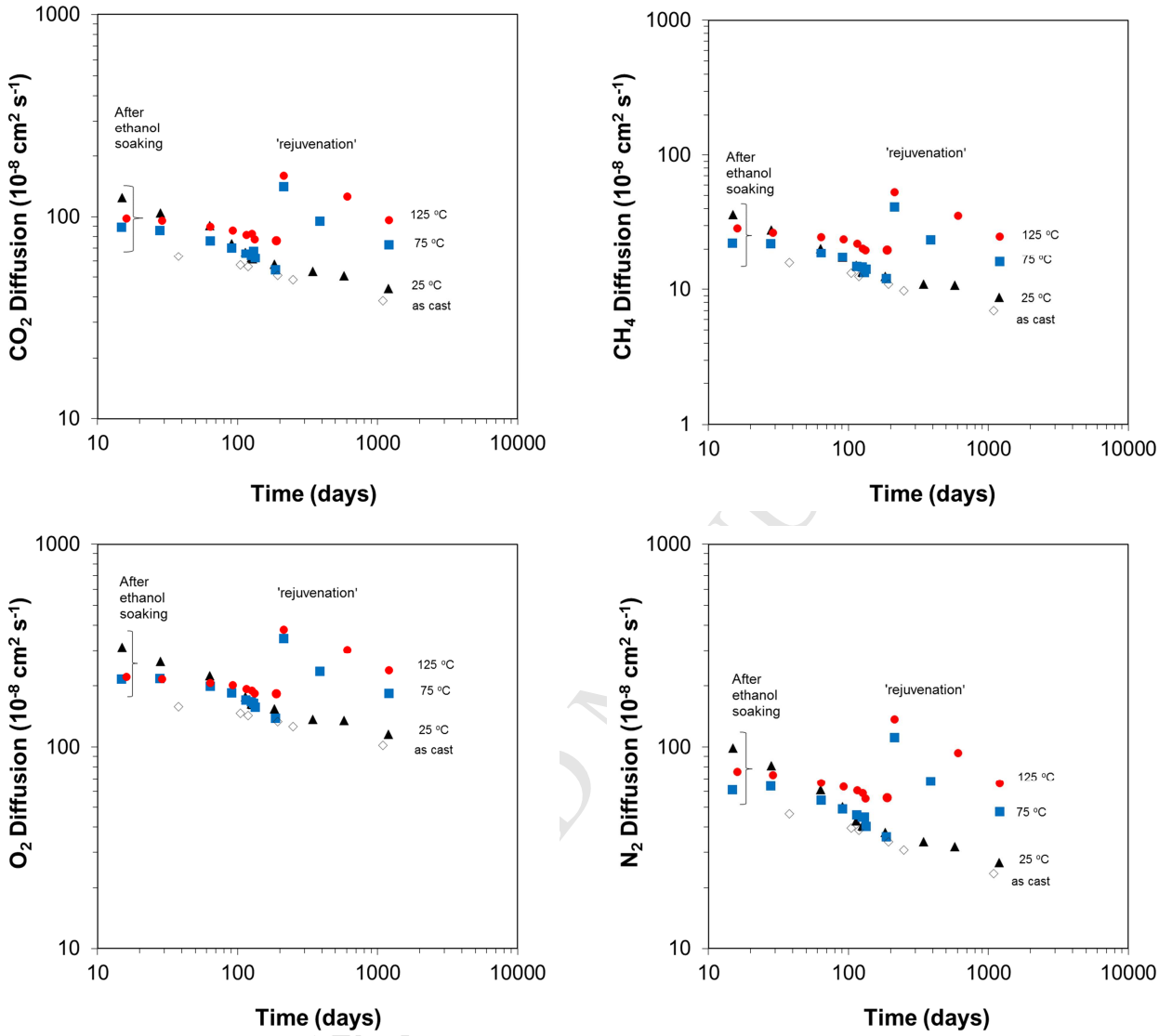

Figure S 3. Diffusivity change at 25°C over time for PIM-1 dense films with different histories as obtained by time lag experiments. Three samples were ethanol soaked and then thermally conditioned at 25 (▲), 75 (■) and 125 °C (●), respectively. An additional sample not treated was followed during time (◇).

Figure S 4 shows the solubility coefficient, *S*, determined indirectly from the equation $S = P / D$. as a function of the aging time for three ethanol soaked samples and an as cast membrane as obtained by time lag measurements.

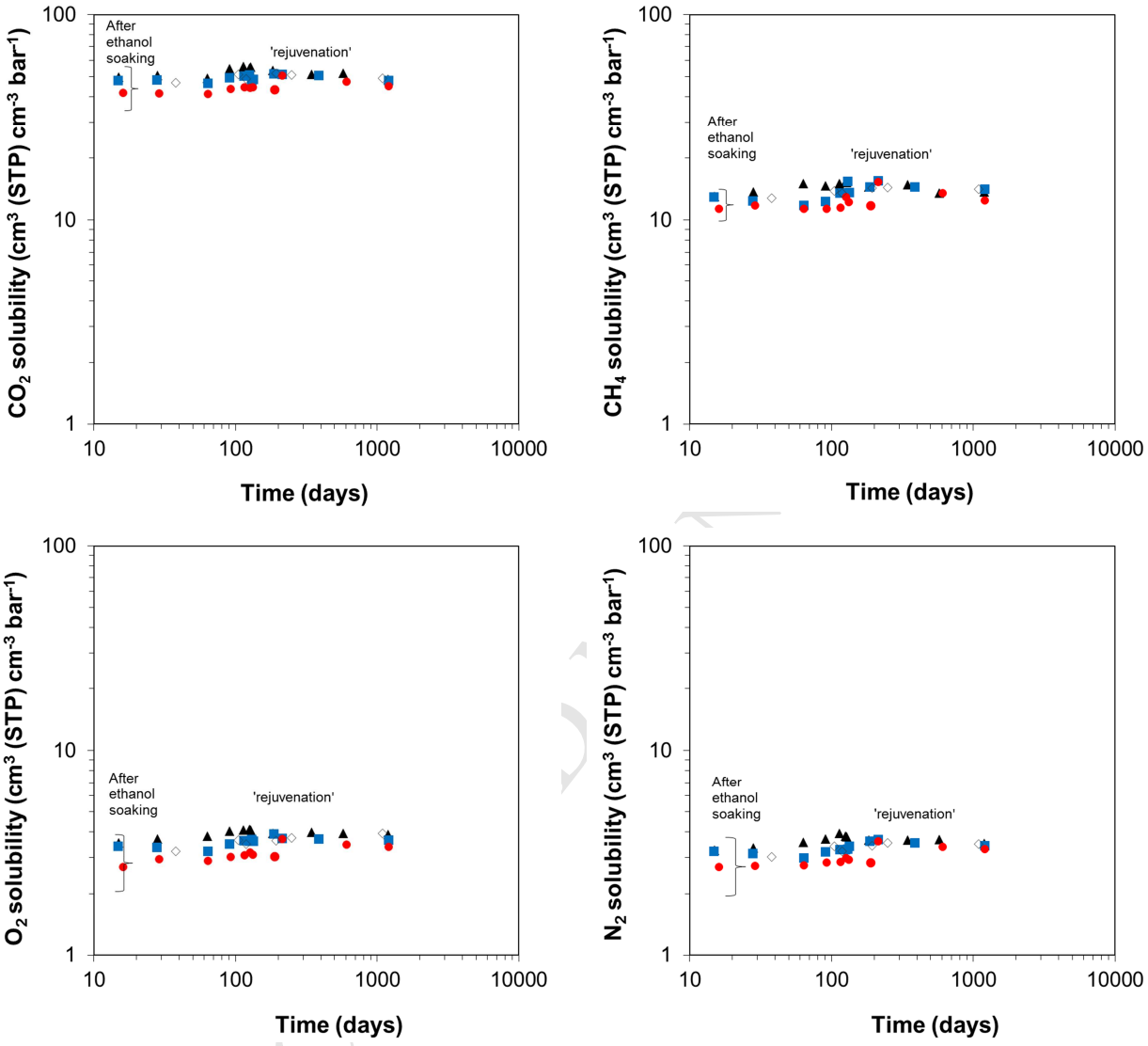

Figure S 4. Solubility change at 25°C over time for PIM-1 dense films with different histories as obtained by time lag experiments. Three samples were ethanol soaked and then thermally conditioned at 25 (▲), 75 (■) and 125 °C (●), respectively. An additional untreated sample was followed during time too (◇).

Sorption

Figure S 5 shows the time dependency of the DMS model parameters, k_D, C'_H and b for the sample after EtOH soaking and thermal treatment at 25°C.

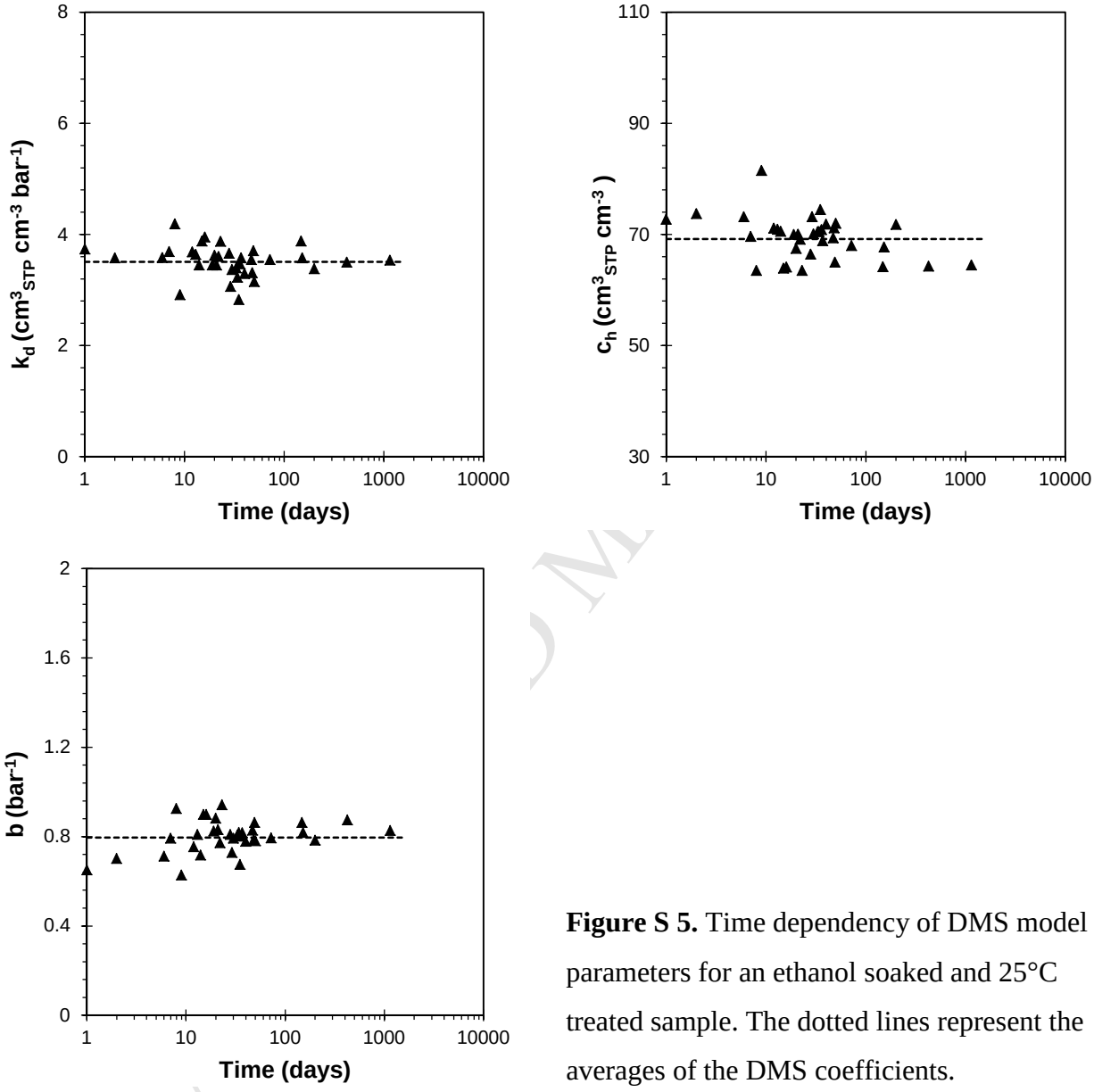

Figure S 5. Time dependency of DMS model parameters for an ethanol soaked and 25°C treated sample. The dotted lines represent the averages of the DMS coefficients.

Figure S 6 shows the change in thickness upon ethanol treatment and subsequent aging for the three films treated at different temperatures after soaking in ethanol.

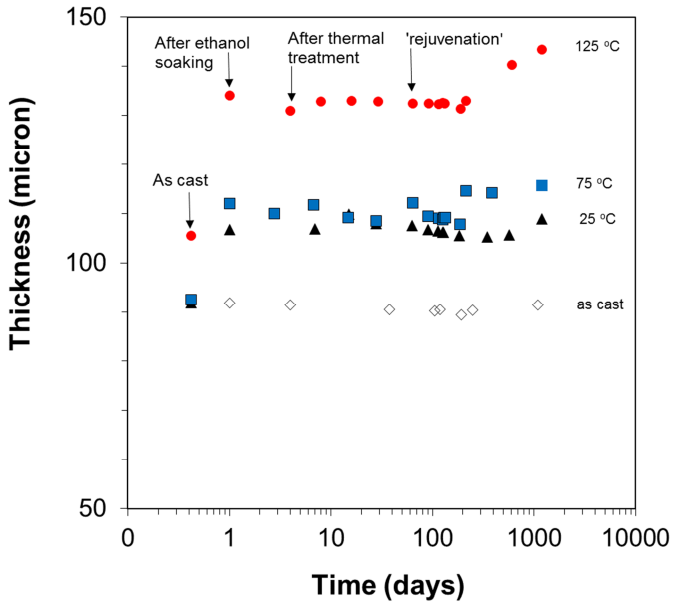

Figure S 6. Effect of the alcohol treatment and the aging on the thickness of PIM-1 films treated at different temperatures after ethanol soaking.

References

[1] T. Emmler, K. Heinrich, D. Fritsch, P.M. Budd, N. Chaukura, D. Ehlers, et al., Free volume investigation of polymers of intrinsic microporosity (PIMs): PIM-1 and PIM1 copolymers incorporating ethanoanthracene units, *Macromolecules*. *43* (**2010**) 6075–6084. doi:10.1021/ma1008786.

Effect of physical aging on the gas transport and sorption in PIM-1 membranes

M. Lanč[1], K. Pilnáček[1], O. Vopička[1], K. Friess[1*], P. Bernardo[2], F. Bazzarelli[2], F. Tasselli[2], G. Clarizia[2], C.R. Mason[3], L. Maynard-Atem[3], P.M. Budd[3*], D. Fritsch[4], Yu.P. Yampolskii[5], V. Shantarovich[6], J.C. Jansen[2*].

Highlights

- The first systematic long-term aging study of PIM-1 membranes by independent sorption and permeation measurements.
- Time lag analysis and gravimetric sorption studies both reveal that aging mainly affects the diffusion coefficient and not the solubility.
- A thermal treatment partially stabilizes the sample against further aging.
- At sufficiently long time scales, the sample properties become almost independent on the previous history.
- Mixed gas permeation experiments confirm excellent separation performance of an aged sample.